Published for SISSA by Springer

Received: *September 5, 2025*
Accepted: *March 2, 2026*
Published: *April 1, 2026*

Measurement of coherent exclusive $J/\psi \to \mu^+\mu^-$ production in ultraperipheral Pb+Pb collisions at $\sqrt{s_{\mathrm{NN}}} = 5.36$ TeV with the ATLAS detector

JHEP04(2026)020

The ATLAS collaboration

Full author list at the end of the paper

E-mail: atlas.publications@cern.ch

Abstract: The ATLAS experiment has performed a measurement of coherent exclusive $J/\psi \to \mu^+\mu^-$ production in ultraperipheral Pb+Pb collisions at $\sqrt{s_{\mathrm{NN}}} = 5.36$ TeV. The data was recorded at the Large Hadron Collider (LHC) during 2023, and corresponds to an integrated luminosity of 79 $\mu\mathrm{b}^{-1}$. Exclusive J/ψ candidates were selected with a dedicated track-sensitive trigger based on the ATLAS transition radiation tracker. The analysis involves reconstruction of the dimuon invariant mass based on muon tracks from the inner detector, as the muon transverse momentum range of interest precludes the use of the standard muon reconstruction and identification algorithms. Differential cross sections are measured as a function of J/ψ rapidity and are compared with theoretical predictions. After extrapolation to $\sqrt{s_{\mathrm{NN}}} = 5.02$ TeV, they are also compared with previous measurements performed by other experiments using data from LHC Run 2. While the results agree reasonably well with theoretical predictions, they are in tension with previous Run-2 results for the central rapidity region.

Keywords: Hadron-Hadron Scattering

ArXiv ePrint: 2509.04135

https://doi.org/10.1007/JHEP04(2026)020

Contents

JHEP04(2026)020

1 Introduction

In ultra-relativistic heavy-ion collisions, the fully-stripped ions are accompanied by large electromagnetic (EM) fields, which correspond to large equivalent photon fluxes, often described in the Weizsäcker-Williams approach [1, 2]. For photons emitted coherently by the entire nucleus, the flux is enhanced compared with beams of protons by a factor of Z^2, where Z is the charge of the nucleus. At large impact parameters, beyond twice the nuclear radius, hadronic processes are suppressed, and photon-induced reactions become the dominant interaction mechanism. Such collisions, referred-to as ultra-peripheral collisions (UPCs), have been used to study photon-nucleus (photonuclear) and photon-photon collisions at the Relativistic Heavy Ion Collider (RHIC) [3] and the Large Hadron Collider (LHC) [4]. Hard-scattering processes in photonuclear interactions provide a novel method for probing nuclear parton distributions in a kinematic region not easily accessible to other measurements [5]. In particular, exclusive diffractive photoproduction of heavy vector mesons is a well-known process that offers unique access to the spatial and momentum structure of the nucleon and nucleus [6, 7]. UPC events typically have features such as rapidity gaps, reduced multiplicity,

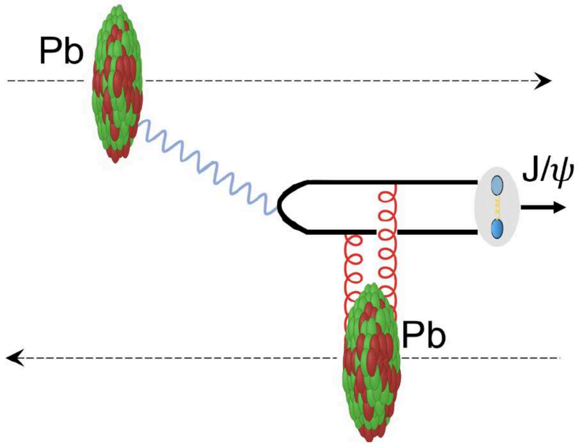

Figure 1. Schematic representation of coherent J/ψ meson photoproduction in Pb+Pb UPC, where a nearly-real photon is emitted from one nucleus, fluctuates to a charm-anticharm dipole, and is put on-shell via scattering from a color-neutral pomeron.

or exclusive final states that make them qualitatively different from the typical hadronic nuclear collisions that are used to study ultra-hot and ultra-dense nuclear matter.

The physics and phenomenology of UPCs, in particular vector meson photoproduction, are reviewed in refs. [8, 9]. Exclusive vector meson photoproduction can proceed in two ways: coherent or incoherent. In coherent photoproduction, the color-neutral exchanged object, typically referred to as a "pomeron", is emitted coherently by all the nucleons in the nucleus and does not directly resolve the nuclear structure, although measurements of this process provide sensitivity to the average nuclear parton distribution function (nPDF). A schematic diagram of the coherent diffractive J/ψ meson photoproduction in UPC is shown in figure 1. In contrast, in incoherent photoproduction, the pomeron is emitted by an individual nucleon, leading to nuclear breakup, or sometimes resolves the nucleon's partonic constituents via dissociative production. Coherent and incoherent exclusive processes can be differentiated experimentally using the magnitude of the transverse momentum (p_{T}) of the produced vector meson, as this quantity is inversely related to the transverse size of the "target", i.e. the object struck by the photon: coherent photoproduction involves the entire nucleus, and typically results in vector mesons with low transverse momentum (of about 50 MeV), while incoherent photoproduction off of nucleons yields mesons with higher transverse momenta (around 250 MeV for nucleons and 600 MeV for dissociative production). In the case of coherent interactions, the nuclei generally remain intact, although the strong EM fields of ultrarelativistic heavy nuclei can induce additional breakup through Coulomb dissociation, causing one or both nuclei to become excited and emit forwardgoing nucleons. Conversely, incoherent photoproduction typically leads to nuclear breakup, sometimes with the emission of additional forward hadrons, which can be misidentified as an exclusive process due to limited detector acceptance.

Coherent exclusive photoproduction of heavy vector mesons (for example, the J/ψ meson) is particularly interesting because, at leading order (LO) in quantum chromodynamics (QCD), the cross section is predicted to scale approximately with the square of the gluon PDF in

JHEP04(2026)020

the target [10]. The scale of the four-momentum transfer of the interaction is related to the mass (m_V) of the vector meson as $Q^2 \approx m_V^2/4$, which implies that the production of heavy charmonium states can be calculated perturbatively. Due to the exclusivity of the reaction, the rapidity of the coherently-produced vector meson is directly related to the Bjorken-x of the gluons as $x = m_V/\sqrt{s_{\mathrm{NN}}}e^{\pm y}$, where y is the rapidity of the vector meson and the two possible signs in the exponent reflect that each of the incoming lead nuclei may act as the photon emitter. At low Bjorken-x values, the nuclear PDFs are well-known to be suppressed compared with those of free protons, a phenomenon referred to as nuclear shadowing [11]. This suppression is generally linked to the multiple scattering effects of a projectile in a nuclear target, and has been explained in various phenomenological approaches [12–17]. Parton saturation phenomena are also expected to emerge at low x. For heavy nuclei such as lead, due to the recombination of gluons at a sufficiently high density, they also reduce the rate of J/ψ production (similar to shadowing), and lead to the emergence of a new momentum scale, Q_s [18]. Heavy vector meson photoproduction measurements thus provide a powerful tool to study shadowing and saturation phenomena. However, the sum of the LO and next-to-leading-order (NLO) gluon contributions exhibits significant cancellations, resulting in a relative dominance of the quark contributions [19]. As a result, this process receives sizable NLO corrections, which complicates the interpretation of coherent exclusive J/ψ production data in terms of gluon shadowing.

Charmonium photoproduction in Pb+Pb UPC has been studied widely by experiments at RHIC [20] and the LHC. Both the ALICE [21–23] and CMS Collaborations [24] have performed measurements at a nucleon-nucleon (NN) center-of mass energy of $\sqrt{s_{\mathrm{NN}}} = 2.76\,\mathrm{TeV}$, in complementary J/ψ rapidity regions. ALICE has performed measurements near midrapidity ($|y| < 0.8$) with both dimuon and dielectron final states, and at forward rapidities $2.5 < y < 4$ with dimuons. CMS has measured the dimuon final state with $1.6 < |y| < 2.4$. In LHC Run-2, with $\sqrt{s_{\mathrm{NN}}} = 5.02\,\mathrm{TeV}$, updated measurements were made by ALICE [25–27] CMS [28], and LHCb [29, 30], the latter in the forward region $2 < y < 4.5$.

This paper presents the measurement of exclusive $J/\psi \to \mu^+\mu^-$ photoproduction cross sections in Pb+Pb UPC at $\sqrt{s_{\mathrm{NN}}} = 5.36\,\mathrm{TeV}$, using 79 $\mu\mathrm{b}^{-1}$ of Run-3 data recorded in 2023. The muons are expected to lose all of their energy in the ATLAS calorimeter material before reaching the muon detectors. Moreover, electrons from the $J/\psi \to e^+e^-$ process are not considered as signal due to the poor electron energy resolution and identification efficiency in the relevant kinematic range. As a result, no specific muon or electron identification criteria are applied. Instead, the analysis relies on the reconstruction of a dimuon invariant mass from a pair of opposite-sign charged particles that are assumed to be muons. After removal of all known backgrounds, the J/ψ cross sections are measured differentially as a function of rapidity within $|y| < 2.5$. This new measurement complements the previous Run-2 measurements by covering a previously-unmeasured region $0.8 < |y| < 1.6$, while also providing measurements in two regions where previous results exist: $|y| < 0.8$ overlapping with ALICE, and $1.6 < |y| < 2.4$ overlapping CMS. The measured cross sections are compared with theory predictions, particularly those which incorporate parton saturation at low Bjorken-x, and the measurements performed at $\sqrt{s_{\mathrm{NN}}} = 5.02\,\mathrm{TeV}$ by the other Collaborations, after a model-dependent extrapolation to account for the beam energy difference.

JHEP04(2026)020

2 Experimental configuration

The ATLAS experiment [31, 32] at the LHC is a multipurpose particle detector with a forward-backward symmetric cylindrical geometry and a near 4π coverage in solid angle.[1] It consists of an inner tracking detector (ID) surrounded by a thin superconducting solenoid providing a 2 T axial magnetic field, electromagnetic and hadronic calorimeters, and a muon spectrometer. The ID covers the pseudorapidity range $|\eta| < 2.5$. It consists of silicon pixel, silicon microstrip, and transition radiation tracking (TRT) detectors. The TRT is the outermost part of the ATLAS ID, and it measures charged particle trajectories before they impinge upon the ATLAS calorimeters. It is divided into four η regions: barrel A ($0 < \eta \lesssim 0.8$), barrel C ($-0.8 \lesssim \eta < 0$), endcap A ($0.8 \lesssim \eta \lesssim 2.0$) and endcap C ($-2.0 \lesssim \eta \lesssim -0.8$). The inner radius of the TRT of about 600 mm makes it sensitive to low-p_{T} charged particles, nominally down to $p_{\mathrm{T}} \approx 0.5$ GeV, below which the curvature of tracks in the ATLAS solenoidal field prevents them from reaching it. Lead/liquid-argon (LAr) sampling calorimeters provide EM energy measurements with high granularity within the region $|\eta| < 3.2$. A steel/scintillator-tile hadronic calorimeter covers the central pseudorapidity range ($|\eta| < 1.7$). The endcap and forward (FCal) regions are instrumented with LAr calorimeters for EM and hadronic energy measurements up to $|\eta| = 4.9$. The muon spectrometer surrounds the calorimeters and is based on three large superconducting air-core toroidal magnets with eight coils each. The field integral of the toroids ranges between 2.0 and 6.0 T m across most of the detector. The muon spectrometer includes a system of precision tracking chambers up to $|\eta| = 2.7$ and fast detectors for triggering up to $|\eta| = 2.4$. The luminosity is measured mainly by the LUCID-2 detector which is located close to the beampipe. Forward neutrons produced from the breakup of lead nuclei in both hadronic and electromagnetic interactions are measured by compact tungsten sampling Zero Degree Calorimeters (ZDCs) positioned at $z = \pm 140$ meters from the ATLAS interaction point.

A two-level trigger system is used to select events [33]. The first-level (L1) trigger is implemented in hardware and uses a subset of the detector information to accept events at a rate close to 100 kHz. This is followed by a software-based trigger that reduces the accepted rate of complete events to 3 kHz on average, depending on the data-taking conditions. A software suite [34] is used in data simulation, in the reconstruction and analysis of real and simulated data, in detector operations, and in the trigger and data acquisition systems of the experiment.

As the final state of $J/\psi \to \mu^+\mu^-$ consists of two soft muons, each with a maximum p_{T} just over 1.5 GeV, the analysis primarily makes use of the ID. In particular, to trigger on the desired final state with two low momentum tracks, the TRT "FastOR" trigger is used at L1 [35].

[1] ATLAS uses a right-handed coordinate system with its origin at the nominal interaction point in the centre of the detector and the z-axis along the beam pipe. The x-axis points from the IP to the centre of the LHC ring, and the y-axis points upwards. Polar coordinates (r, ϕ) are used in the transverse plane, ϕ being the azimuthal angle around the z-axis. The pseudorapidity is defined in terms of the polar angle θ as $\eta = -\ln\tan(\theta/2)$ and is equal to the rapidity $y = \frac{1}{2}\ln\left(\frac{E+p_z}{E-p_z}\right)$ in the relativistic limit. Angular distance is measured in units of $\Delta R \equiv \sqrt{(\Delta y)^2 + (\Delta\phi)^2}$.

The L1 TRT trigger logic is illustrated in figure 2 for the TRT barrel A region. The trigger is derived from a logical OR of fast electronic signals, reflecting the passage of tracks through the straw tubes. The TRT straw tubes are connected to the readout electronics via front-end modules which each process signals from 16 straws. Each TRT front-end module can be configured to send a signal that is generated using a fast digital OR circuit (FastOR) to the TRT trigger timing and control (TTC) board if a hit exceeding a high threshold level (HT) is recorded in at least one of its associated straws. A logic circuit on the TTC board aggregates these signals from groups of several front-end chips, which reflect contiguous azimuthal regions. If the number of received signals within a TTC board exceeds a configurable threshold, set to four in 2023 Pb+Pb collisions, a trigger signal is generated for the region. All four TRT regions provide a similar binary trigger signal, which are logically OR'ed to provide a fast binary trigger decision for each event.

Until 2023, the L1 TRT trigger had been used primarily for cosmic ray triggering in ATLAS. For the 2023 heavy-ion run, it was re-deployed with some operational modifications to provide triggering on final states with up to $\mathcal{O}(10)$ low-p_{T} tracks. Due to high hit occupancy, the L1 TRT trigger is unsuitable for nominal proton-proton (pp) collisions and is only viable in low-pileup conditions such as cosmic-ray or Pb+Pb runs. Typically, the TRT HT level is calibrated to the transition radiation threshold and is used for electron identification [36]. In Pb+Pb collisions, this was lowered to about twice the low threshold used in the standard pp tracking algorithms [36], such that a typical charged particle reaching the TRT can produce a large number of HT hits. In this way, the TRT was able to trigger on events with even just one or two low-momentum tracks.

3 Data and Monte Carlo simulation samples

The data used in this measurement were recorded by ATLAS in 2023 during Pb+Pb operation of the LHC at $\sqrt{s_{\mathrm{NN}}} = 5.36$ TeV. To accumulate $J/\psi \to \mu^+\mu^-$ events with a good efficiency while rejecting hadronic heavy ion collisions, candidate events were recorded using a dedicated trigger for events with moderate activity in the ID but little additional activity in the entire detector. The L1 decision required both a signal from the L1 TRT FastOR system and a total transverse energy (E_{T}) below 20 GeV (at electromagnetic scale) registered in the calorimeter system. At the HLT, the total E_{T} in the FCal region on each side was required to be below 5 GeV, to suppress hadronic events. In addition, the ID was used at the HLT to select events with up to 15 tracks with $p_{\mathrm{T}} > 100$ MeV, with an additional requirement of 1–5 tracks with $p_{\mathrm{T}} > 1$ GeV. The efficiency of the trigger selection is described in section 7. The trigger was prescaled at L1 during the data-taking period (meaning that not every event that satisfied the trigger requirements was recorded for further processing). The data set corresponds to an integrated luminosity of 79 $\mu\mathrm{b}^{-1}$.

Monte Carlo (MC) simulated events for the coherent UPC $J/\psi \to \mu^+\mu^-$ process were produced using version 2.0 of the STARlight generator [37] interfaced with Pythia 8.312 [38] to model final-state radiation (FSR) from the muons [39]. For the $J/\psi \to \mu^+\mu^-$ process, STARlight relies on the vector meson dominance (VMD) model and utilizes a parameterization of existing data on J/ψ photoproduction off protons. To determine the J/ψ photoproduc-

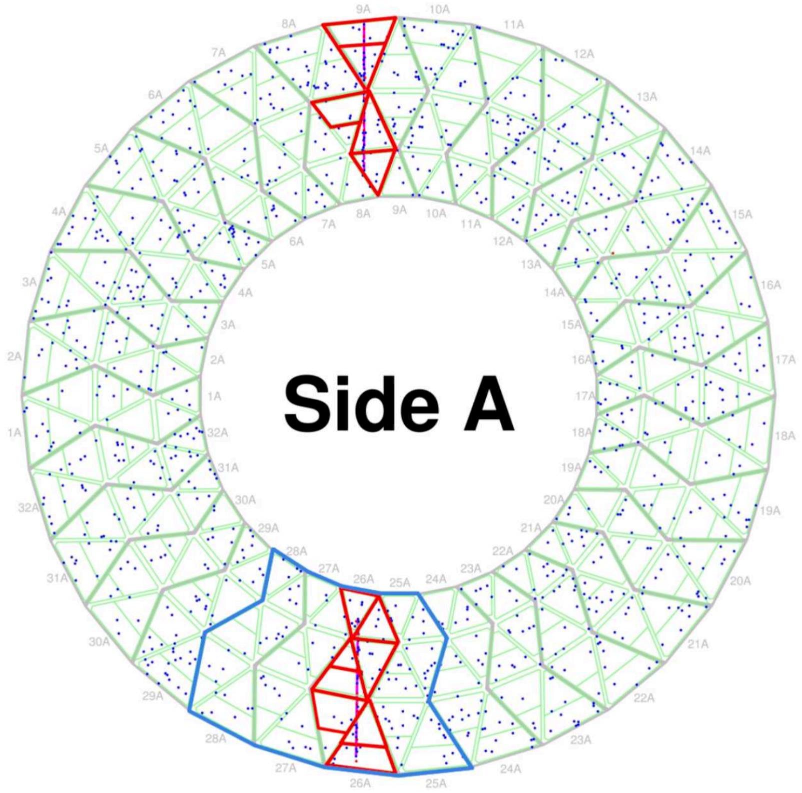

Figure 2. The L1 TRT trigger logic in the TRT barrel A region ($0 < \eta \lesssim 0.8$) [35]. The region is divided into 32 ϕ sectors (bold gray), each consisting of nine TRT trigger segments (shown as green triangles and trapezoids). A trigger signal within a segment is formed if the transition radiation threshold is exceeded in any of TRT straws from this segment (shown as red triangles and trapezoids, induced by a vertical cosmic track in this event). The trigger logic then aggregates signals from all segments in a region formed from four adjacent ϕ sectors (shown in blue), yielding an effective ϕ segmentation of $2\pi/8$. To form a trigger decision for this TRT section, the number of segments with a trigger signal has to exceed a fixed threshold multiplicity ($M = 4$) in at least one contiguous set of four sectors.

JHEP04(2026)020

tion cross section in Pb+Pb UPC, a Glauber formalism is applied that considers multiple interactions within the nucleus but does not include explicit gluon-shadowing corrections.

The sources of background in this analysis include coherent $J/\psi \to e^+e^-$, incoherent $J/\psi \to \ell^+\ell^-$, coherent and incoherent ψ(2S), and $\gamma\gamma \to \ell^+\ell^-$ processes, where $\ell = e, \mu$. These backgrounds were also modeled with STARlight. It was similarly interfaced to Pythia 8 for coherent $J/\psi \to e^+e^-$, incoherent $J/\psi \to \ell^+\ell^-$ and $\gamma\gamma \to \ell^+\ell^-$ UPC production. The feed-down background from the production of coherent and incoherent ψ(2S) vector meson in UPC was generated with STARlight, and EvtGen 2.2.1 [40] was used to provide all known $\psi(2S)$ decay channels. The FSR from the charged decay products of ψ(2S) vector mesons was simulated with Photos++ 3.61 [41].

In all of the STARlight events, the produced J/ψ and ψ(2S) vector mesons were assumed to be transversely polarized. This is consistent with expectations from helicity conservation in photoproduction processes and is also consistent with experimental observations [42].

The generated p_{T} distribution of coherent J/ψ from STARlight is reweighted to match the measured cross sections by the LHCb Collaboration [30]. The measured coherent J/ψ p_{T} shape from LHCb is found to be consistent with the shape measured by ALICE at mid-rapidity [43]. This reweighting procedure leads to corrections at the level of approximately 10–20% in the J/ψ p_{T} spectrum and significantly improves the modeling of the J/ψ p_{T} shape in the entire rapidity range.

4 Signal selection

The selected signal events are required to have exactly two, opposite-charge tracks. Charged-particle tracks are reconstructed in the ID using an algorithm optimized for pp minimum-bias measurements [44]. They are pre-selected to have $p_{\mathrm{T}} > 100$ MeV and $|\eta| < 2.5$, and to have a transverse impact parameter calculated relative to the measured beam-line position of $|d_0| < 2$ mm. The Loose Primary track selection [45–47] is used to reject poorly-reconstructed tracks.

Apart from the track veto (exactly two tracks with $p_{\mathrm{T}} > 100\,\mathrm{MeV}$ and $|\eta| < 2.5$), no other exclusivity selection criteria are applied. However, various cross-checks are performed (see section 8.4) to ensure that the selected events are produced without additional hadronic activity. These cross-checks also ensure that the applied exclusivity selection criteria are insensitive to potential biases arising from additional UPC interactions occurring in the same or in separate Pb+Pb collisions.

In addition, the p_{T} of both tracks is required to be above 1 GeV to coincide with the trigger requirements. The muon mass hypothesis is used for each track. Due to the very low p_{T} of the muons from the J/ψ decay, no specific identification criteria are used, as these particles are expected to lose all their energy and stop in the calorimeter before they can reach the muon detectors. The signal region (SR) selection then requires the invariant mass of the two-track system to be in the range of $2.9 < m_{\mu^+\mu^-} < 3.2\,\mathrm{GeV}$, and the pair transverse momentum to be $p_{\mathrm{T}}^{\mu^+\mu^-} < 0.2\,\mathrm{GeV}$. A small $p_{\mathrm{T}}^{\mu^+\mu^-}$ is required because coherent photoproduction involves the entire nucleus and thus imparts very little transverse momentum to the J/ψ.

5 Background estimate and signal yield extraction

This section summarizes the estimations of the primary background sources, and the signal yield extraction procedure. The main sources of background are the $\gamma\gamma \to \ell^+\ell^-$ and $J/\psi \to e^+e^-$ processes. Other sources of background are the incoherent $J/\psi \to \ell^+\ell^-$ process, coherent and incoherent $\psi(2\mathrm{S})$ production, and a combinatorial background of pion pairs from inelastic photonuclear processes.

5.1 $\psi(2\mathrm{S})$ feed-down

Photoproduced $\psi(2\mathrm{S})$ mesons can decay to $J/\psi + X$, where X denotes additional particles (typically soft pions), which can go undetected due to the limited ID acceptance in η or p_{T}, and material interactions that preclude their reconstruction. Yields of these events are estimated with MC simulations, with an additional normalization factor extracted from a control region. This control region selects events with a $\psi(2S) \to J/\psi(\to \ell^+\ell^-)\pi^+\pi^-$ decay and it requires:

- exactly three or four tracks, where the leading (subleading) track has $p_T > 1$ GeV ($p_T > 0.8$ GeV) and the two leading tracks have opposite charge;
- the third-leading track has $p_T > 0.2$ GeV;
- if exactly three tracks are present, exactly one pixel track[2] unmatched with the other three tracks (with a ΔR(track, pix. track) < 0.4 matching condition) is required, and is also called a *track* in the following; then, the 3rd and 4th leading tracks are also required to have opposite charge;
- the invariant mass of the two leading tracks to satisfy $3 < m_{\mu^+\mu^-} < 3.2$ GeV, and the invariant mass of the full system to satisfy $3.5 < m_{\mu^+\mu^-\pi^+\pi^-} < 3.8$ GeV, where the charged pion mass hypothesis is used for the 3rd and 4th leading tracks;
- the acoplanarity ($A_\phi = 1 - |\Delta\phi|/\pi$) between the leading and subleading track system, and the 3rd and 4th leading track system, $A_\phi(\mu^+\mu^-, \pi^+\pi^-) < 0.5$.

The dominant background for this $\psi(2S)$ decay process comes from combinatorial processes (multiple pion production) and is estimated by using events from $m_{\mu^+\mu^-}$ low-mass ($2.6 < m_{\mu^+\mu^-} < 2.75$ GeV) and high-mass ($3.25 < m_{\mu^+\mu^-} < 3.4$ GeV) sidebands. Other background includes $J/\psi\rho^0$ production, and it is estimated by using a dedicated control region. First, the $A_\phi(\mu^+\mu^-, \pi^+\pi^-) < 0.5$ requirement is inverted. This is because the $J/\psi\rho^0$ background is flat with $A_\phi(\mu^+\mu^-, \pi^+\pi^-)$, whereas $\psi(2S) \to J/\psi(\to \ell^+\ell^-)\pi^+\pi^-$ events concentrate at low $A_\phi(\mu^+\mu^-, \pi^+\pi^-)$ values. Then, additional requirements of $A_\phi(\mu^+, \mu^-) < 0.02$ and $A_\phi(\pi^+, \pi^-) < 0.1$ are used to reflect the fact that J/ψ and ρ^0 decays are from two separate photonuclear processes, even when produced by the same Pb+Pb interaction. Moreover, the $3.5 < m_{\mu^+\mu^-\pi^+\pi^-} < 3.8$ GeV requirement is relaxed to $m_{\mu^+\mu^-\pi^+\pi^-} < 4$ GeV.

To extract the coherent and incoherent $\psi(2S)$ components, a fit to the four-track system p_T distribution is performed, with the normalization factors for the two components as free parameters. These factors are then used to normalize the coherent and incoherent $\psi(2S)$ MC samples, which are subsequently used to estimate the $\psi(2S)$ background in the SR.

5.2 Pions from inclusive photonuclear events

As the analysis does not use any specific identification criteria for muons, a combinatorial background from hadronic photonuclear events is expected. In such events, a photon fluctuates into a hadronic state, typically a ρ^0, and interacts with the nucleus to form a multi-hadron final state. This can lead to events in which only a few particles are observed in the ID. The contribution of these events to the SR is estimated by using a data-driven procedure using same-sign track pairs. Template $p_T^{\mu^\pm\mu^\pm}$ distributions are obtained from events satisfying all

[2]Pixel tracks are reconstructed using hits from the pixel detector only. They are required to have $p_T > 50$ MeV, $|\eta| < 2.5$, and at least three hits in the pixel detector. As pixel tracks provide much better reconstruction efficiency at $p_T \sim 100$ MeV relative to full ID tracks, and because the pions from $\psi(2S) \to J/\psi(\to \ell^+\ell^-)\pi^+\pi^-$ are very soft, this procedure significantly improves the $\psi(2S)$ selection efficiency.

JHEP04(2026)020

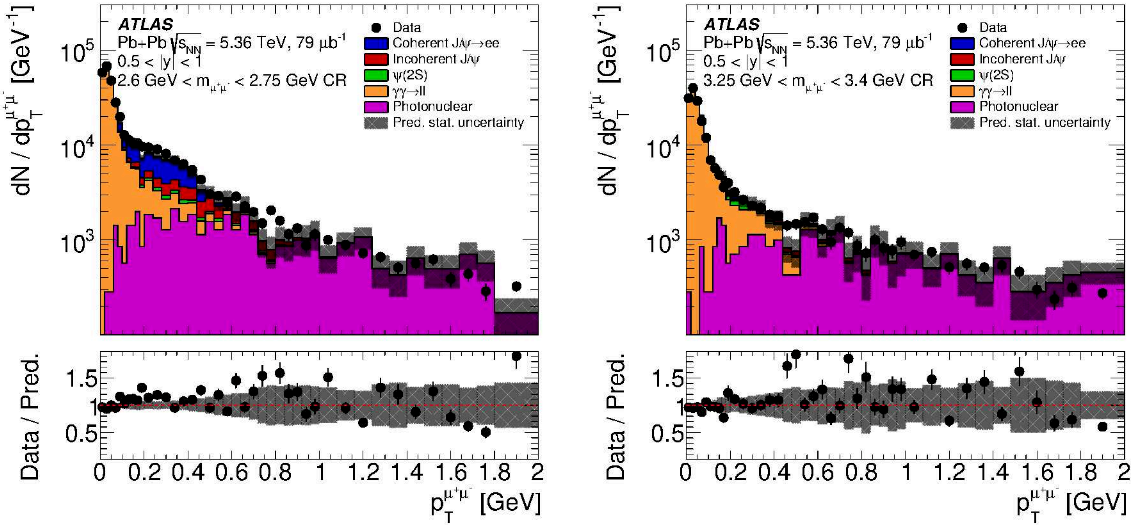

(a) (b)

Figure 3. Observed exclusive two-track system p_T distributions together with fit signal and background contributions in the rapidity range $0.5 < |y| < 1$ for the (a) low-mass ($2.6 < m_{\mu^+\mu^-} < 2.75$ GeV) and (b) high-mass ($3.25 < m_{\mu^+\mu^-} < 3.4$ GeV) sideband regions. The photonuclear background templates are normalized in the low-mass sideband region in the $p_\mathrm{T}^{\mu^+\mu^-} > 1$ GeV range. The signal contribution (coherent $J/\psi \to \mu^+\mu^-$) is negligible in these two regions and hence it is not shown. For the calculation of $p_\mathrm{T}^{\mu^+\mu^-}$, the muon mass hypothesis is used for each track.

signal selection criteria except the opposite-sign requirement, which is inverted. Templates are derived in the range of $p_\mathrm{T}^{\mu^\pm\mu^\pm} < 2$ GeV, for the SR ($2.9 < m_{\mu^+\mu^-} < 3.2$ GeV), and for both the low-mass ($2.6 < m_{\mu^+\mu^-} < 2.75$ GeV) and high-mass ($3.25 < m_{\mu^+\mu^-} < 3.4$ GeV) sideband regions. These photonuclear background templates are then normalized in the low-mass sideband region for events having $p_\mathrm{T}^{\mu^+\mu^-} > 1$ GeV where other contributions ($\gamma\gamma \to \ell^+\ell^-$, $J/\psi \to \ell^+\ell^-$) are found to be suppressed. This normalization is shown in figure 3(a) for a representative J/ψ rapidity bin. As a cross-check of the full procedure, the high-mass sideband region is shown in figure 3(b), where a good agreement between the data and background estimate is observed, using the results from the low-mass fit.

5.3 $m_{\mu^+\mu^-}$ fits for $\gamma\gamma \to \ell^+\ell^-$ and J/ψ processes

Electrons from the $J/\psi \to e^+e^-$ process experience significant detector distortions due to energy loss and radiative processes in the ID material, resulting in broadened and shifted mass peaks compared with the $J/\psi \to \mu^+\mu^-$ decay. To discriminate between the $J/\psi \to \mu^+\mu^-$, $J/\psi \to e^+e^-$ and $\gamma\gamma \to \ell^+\ell^-$ processes, template fits to the two-track invariant mass spectra for SR events in the extended two-track invariant mass range of $2.5 < m_{\mu^+\mu^-} < 3.5$ GeV, are performed. The $J/\psi \to \ell^+\ell^-$ process considered here includes a sum of coherent, incoherent and ψ(2S) feed-down contributions. The fits use the following inputs:

- $J/\psi \to \mu^+\mu^-$ and $J/\psi \to e^+e^-$ mass shapes described by double-sided Crystal Ball functions [48], whose parameters are fixed using fits to simulated events,

JHEP04(2026)020

- a small contribution from pions from inclusive photonuclear events modeled using same-sign templates from data, as explained in section 5.2, and further smoothed using an exponential function ($e^{p_0+p_1\cdot m}$, where p_0 and p_1 are the fit parameters),

- an exponential function describing the $\gamma\gamma \to \ell^+\ell^-$ background process, with a floating slope parameter.

In total, this results in four fit parameters for each rapidity interval: normalization factors for $J/\psi \to \mu^+\mu^-$ and $J/\psi \to e^+e^-$ contributions and two parameters for the $\gamma\gamma \to \ell^+\ell^-$ background (slope and normalization). Binned maximum-likelihood fits are performed in each two-track rapidity interval, with results shown in figure 4. The fits well describe the two-track invariant mass spectra observed in data, with a chi-squared per degree of freedom for each distribution in the range of 0.8–1.3.

The suppression of the $J/\psi \to e^+e^-$ contribution at higher $|y|$ regions, as shown in figure 4, is attributed to the increased amount of ID material with $|\eta|$, which affects both the track reconstruction efficiency and the momentum reconstruction for electrons. It is worth noting that the ratio of the fitted $J/\psi \to e^+e^-$ and $J/\psi \to \mu^+\mu^-$ yields is consistent with the ratio predicted by the MC simulation within 20% across the entire rapidity range.

To cross-check the absolute rate of the $\gamma\gamma \to \ell^+\ell^-$ background process, events in the low-mass and high-mass sideband regions are examined. The $\gamma\gamma \to \ell^+\ell^-$ predictions, normalized using cross sections from STARlight, are below the observed yields by approximately 20%. This discrepancy is consistent with previous observations of the $\gamma\gamma \to \ell^+\ell^-$ process in Pb+Pb UPC at low dilepton invariant masses [22, 49, 50].

5.4 Dissociative incoherent $J/\psi \to \ell^+\ell^-$ production

Incoherent $J/\psi \to \ell^+\ell^-$ production with nucleon dissociation is also taken into account to describe the high-$p_{\mathrm{T}}^{\mu^+\mu^-}$ tail with the template based on the parameterization used by the H1 Collaboration [51]. The differential proton-dissociative cross section is parameterised, as a function of $p_{\mathrm{T}}^{\mu^+\mu^-}$, with a power-law function $d\sigma/dp_{\mathrm{T}} \approx p_{\mathrm{T}}(1+(b_{pd}/n)p_{\mathrm{T}}^2)^{-n}$. The parameters are set to $n = 3.58$ and $b_{pd} = 1.79\,\mathrm{GeV}^{-2}$, according to fits to $\gamma p \to J/\psi X$ data [51]. This functional form has also been used in previous ALICE and CMS measurements [25–28].

5.5 Yield extraction fits to $p_{\mathrm{T}}^{\mu^+\mu^-}$

The raw exclusive UPC J/ψ yields obtained from the invariant mass fits contain contributions from coherent and incoherent J/ψ photoproduction that can be separated via the analysis of the $p_{\mathrm{T}}^{\mu^+\mu^-}$ spectra.

Individual $p_{\mathrm{T}}^{\mu^+\mu^-}$ distributions are fit in the signal region $2.9 < m_{\mu^+\mu^-} < 3.2\,\mathrm{GeV}$ with MC templates produced using the simulated STARlight samples, corresponding to the production mechanisms discussed above: coherent and incoherent $J/\psi \to \ell^+\ell^-$, feed-down $J/\psi \to \ell^+\ell^-$ from decays of coherent and incoherent $\psi(2S)$ and the dilepton continuum from the $\gamma\gamma \to \ell^+\ell^-$ process (both to dimuons and dielectrons). In addition, pions from inclusive photonuclear events are included using the $p_{\mathrm{T}}^{\mu^+\mu^-}$ templates obtained from same-sign events.

In these fits, the normalizations of the templates for $\psi(2S)$ feed-down and photonuclear pion pairs are kept fixed according to the procedures explained in sections 5.1 and 5.2. The

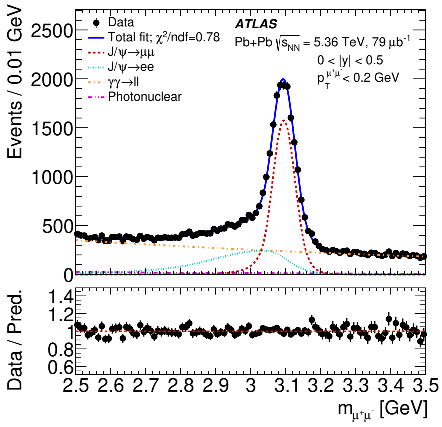

(a)

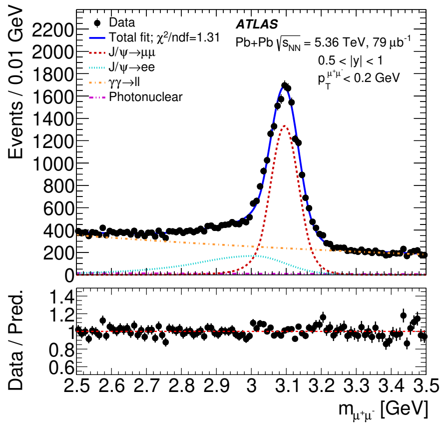

(b)

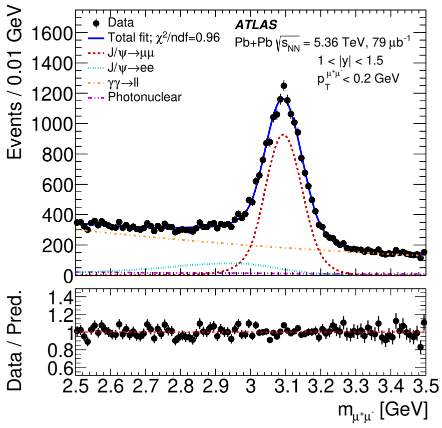

(c)

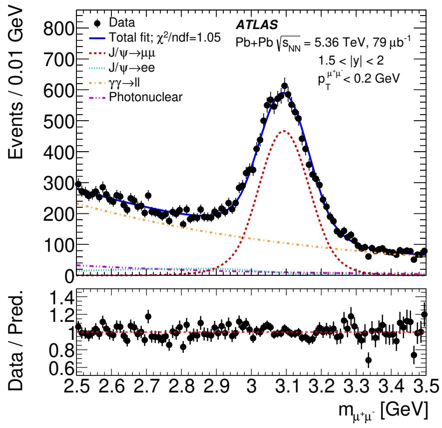

(d)

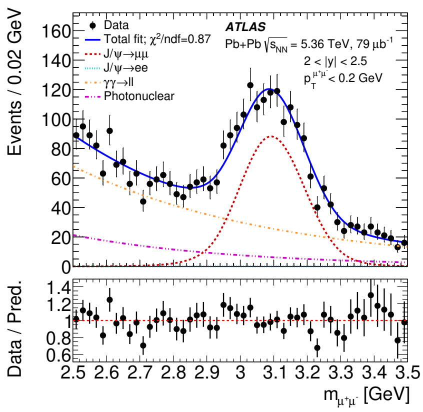

(e)

Figure 4. Exclusive two-track invariant mass ($m_{\mu^+\mu^-}$) distributions for five $|y|$ intervals. Resonant contributions from $J/\psi \to \mu^+\mu^-$ and $J/\psi \to e^+e^-$ processes are shown as long-dashed and short-dashed lines, respectively. Non-resonant contributions from $\gamma\gamma \to \ell^+\ell^-$ and photonuclear backgrounds are shown as dotted-dashed and two-dotted dashed lines respectively. The total fit result for each rapidity region is shown as a solid line. The bottom panel in each figure shows the ratio of data to the total prediction. For the calculation of $m_{\mu^+\mu^-}$, the muon mass hypothesis is used for each track. The signal region is defined as $2.9 < m_{\mu^+\mu^-} < 3.2\,\text{GeV}$.

JHEP04(2026)020

normalization of the dilepton continuum from the $\gamma\gamma \to \ell^+\ell^-$ process is fixed by the results for the background description of the two-track invariant mass fits. In addition, the $e^+e^-/\mu^+\mu^-$ ratios for individual contributions are kept fixed according to the results from the invariant mass fits. Hence, the only free parameters in the $p_{\mathrm{T}}^{\mu^+\mu^-}$ fits are the normalization factors for coherent $J/\psi \to \ell^+\ell^-$, incoherent $J/\psi \to \ell^+\ell^-$, and dissociative incoherent $J/\psi \to \ell^+\ell^-$ production. For each rapidity interval, the binned maximum-likelihood fits are performed for events in the $0 < p_{\mathrm{T}}^{\mu^+\mu^-} < 2\,\mathrm{GeV}$ range. Figure 5 shows the $p_{\mathrm{T}}^{\mu^+\mu^-}$ distributions after the fit procedure. The combined templates adequately describe the $p_{\mathrm{T}}^{\mu^+\mu^-}$ shapes observed in data.

While there is some overlap between events used in the invariant mass and $p_{\mathrm{T}}^{\mu^+\mu^-}$ fits, the impact of residual correlations is found to be negligible, as the incoherent J/ψ contribution is small (a few percent in the signal region) and is primarily constrained by the high-$p_{\mathrm{T}}^{\mu^+\mu^-}$ tail, which lies outside the mass fit selection.

6 Efficiency and acceptance corrections

The coherent J/ψ meson differential cross section is given by

$$\frac{\mathrm{d}\sigma}{\mathrm{d}y} = \frac{N^{\mathrm{coh}}_{J/\psi\to\mu^+\mu^-}}{A \times \epsilon_C \times BR \times \mathcal{L}_{\mathrm{int}} \times \Delta y}\,, \tag{6.1}$$

where Δy denotes the rapidity interval, $\mathcal{L}_{\mathrm{int}}$ is the integrated luminosity of the data sample, BR is the $J/\psi \to \mu^+\mu^-$ branching fraction, ϵ_C and A denote the efficiency and acceptance corrections, respectively, and $N^{\mathrm{coh}}_{J/\psi\to\mu^+\mu^-}$ is the raw yield of coherent $J/\psi \to \mu^+\mu^-$ events extracted from the $p_{\mathrm{T}}^{\mu^+\mu^-}$ fits. The correction factor ϵ_C accounts for detector inefficiencies, which can be factorized into reconstruction efficiency and trigger efficiency components (the latter discussed in detail in section 7). It is defined as the ratio of the number of generated events that satisfy the final selection criteria after event reconstruction to the number of generated events within the fiducial region. The fiducial region is defined as two muons (after FSR) having $p_{\mathrm{T}}^{\mu} > 1\,\mathrm{GeV}$, $|\eta^{\mu}| < 2.5$, $2.9 < m_{\mu^+\mu^-} < 3.2\,\mathrm{GeV}$ and $p_{\mathrm{T}}^{\mu^+\mu^-} < 0.2\,\mathrm{GeV}$. The factor A is the acceptance for coherent $J/\psi \to \mu^+\mu^-$ within the fiducial region. It is defined, using STARlight MC, as the fraction of generated events in the given J/ψ rapidity interval and before the emission of FSR from the decay muons (QED Born level) that satisfy the fiducial requirements. This acceptance is determined entirely using the MC signal sample and is used to extrapolate the measured cross section in the fiducial region to the full phase space. The migration between the individual y bins is found to be below 0.5%.

Table 1 shows the numerical values of ϵ_C and A. The values of ϵ_C vary between 64% and 78% for $|y| < 2$. For the $2 < |y| < 2.5$ rapidity bin, $\epsilon_C \approx 22\%$. Similarly, the values of A are in the range of 51–63% for $|y| < 2$ region and around 19% for the $2 < |y| < 2.5$ region. The acceptance loss comes mainly from the ID pseudorapidity coverage ($|\eta^{\mu}| < 2.5$ requirement).

7 Trigger efficiency measurement

The efficiency of the L1 TRT trigger is determined using an independent set of triggers based on a ZDC selection at L1. The supporting ZDC trigger selects events having ZDC activity consistent with the presence of at least one neutron on either side and none on the

JHEP04(2026)020

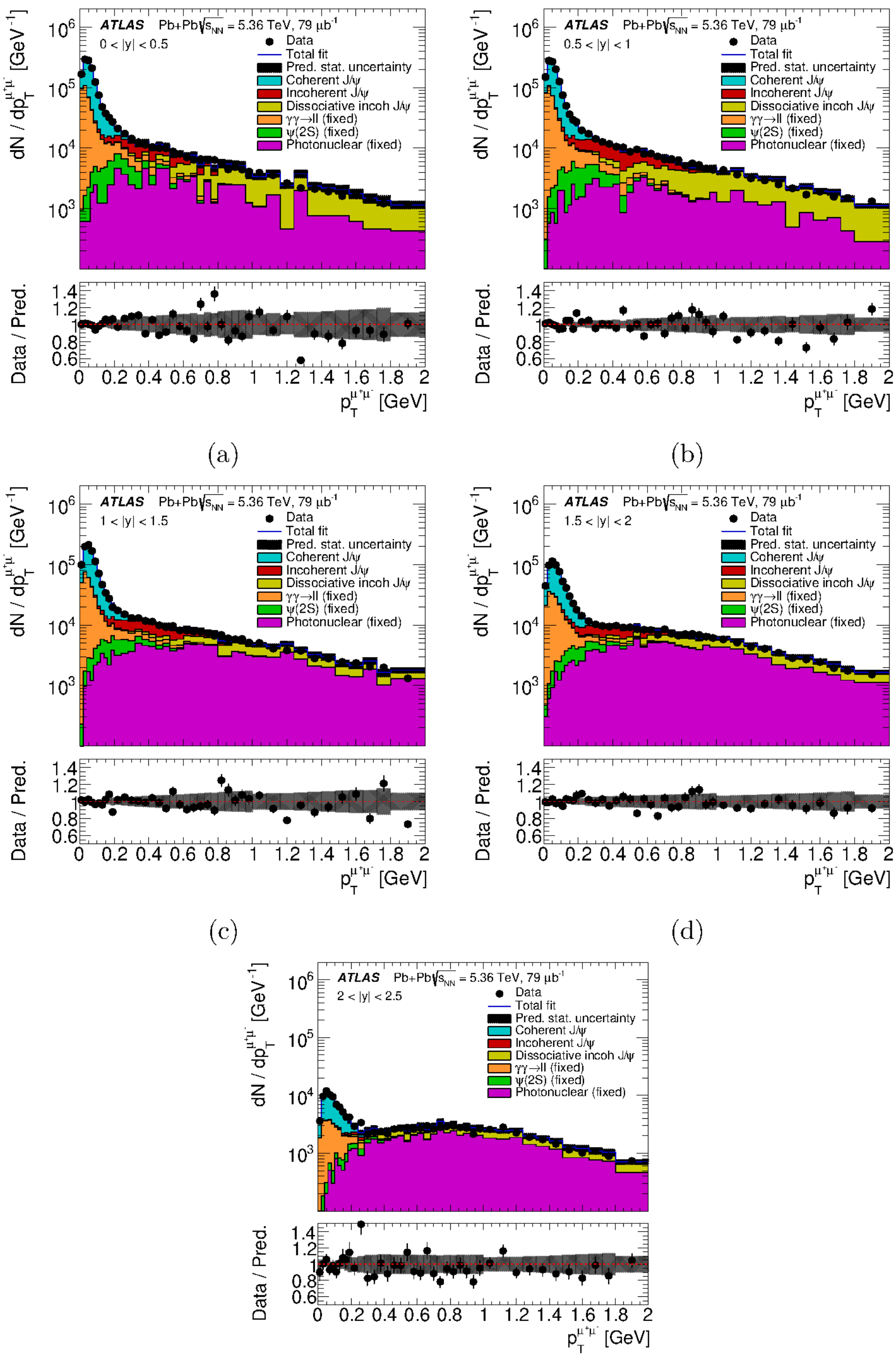

(e)

Figure 5. Demonstration of the coherent J/ψ signal yield extraction. The exclusive two-track system p_{T} distributions in the SR, after relaxing the $p_{\mathrm{T}}^{\mu^+\mu^-} < 0.2\,\mathrm{GeV}$ requirement, are fit using templates from simulation, as described in the text. The fits are performed separately in (a–e) five $|y|$ intervals. The total fit result for each rapidity region is shown as a solid blue line. Individual contributions to the fit are shown using different colors. The bottom panel in each figure shows the ratio of data to the total fit. For the calculation of $p_{\mathrm{T}}^{\mu^+\mu^-}$, the muon mass hypothesis is used for each track.

Rapidity range	A	ϵ_C
$\|y\| < 0.5$	0.633 ± 0.002 (stat.)	0.722 ± 0.002 (stat.) ± 0.016 (syst.)
$0.5 < \|y\| < 1$	0.632 ± 0.002 (stat.)	0.776 ± 0.002 (stat.) ± 0.013 (syst.)
$1 < \|y\| < 1.5$	0.633 ± 0.002 (stat.)	0.720 ± 0.002 (stat.) ± 0.020 (syst.)
$1.5 < \|y\| < 2$	0.510 ± 0.002 (stat.)	0.643 ± 0.003 (stat.) ± 0.020 (syst.)
$2 < \|y\| < 2.5$	0.186 ± 0.001 (stat.)	0.227 ± 0.002 (stat.) ± 0.019 (syst.)

Table 1. Summary of efficiency and acceptance correction factors.

opposite side, accompanied by a total maximum transverse energy of 200 GeV. At the HLT, a 5 GeV maximum transverse energy in each FCal region, and at least one track in the ID with $p_{\mathrm{T}} > 200$ MeV, are required. These triggers are sensitive to coherent $J/\psi \to \mu^+\mu^-$ events with single electromagnetic dissociation of one of the outgoing ions [27]. The ZDC triggers are fully independent of the ID, and thus serve as an unbiased reference for the L1 TRT trigger.

The offline event selections for the L1 TRT trigger efficiency evaluation are similar to that used in the actual $J/\psi \to \mu^+\mu^-$ analysis. To extract the L1 TRT trigger efficiency for muon pairs from $J/\psi \to \mu^+\mu^-$ decay, fits to the 2-track invariant mass distributions are performed, similar to the nominal signal analysis (section 5.3).

The L1 TRT trigger efficiency has a significant dependence on the track $|\eta|$, reflecting the physical structure of the TRT. To take this into account, the efficiency is derived in two dimensions, in bins of $|\eta_1|$ and $|\eta_2|$, where $|\eta_1|$ ($|\eta_2|$) denotes the absolute pseudorapidity of a track with lower (higher) $|\eta|$ value. The efficiency is studied in six $|\eta|$ regions: $|\eta| < 0.7$, corresponding to the TRT barrel region; $0.7 \leq |\eta| < 0.9$ and $0.9 \leq |\eta| < 1.1$, corresponding to the transition region; $1.1 \leq |\eta| < 1.8$, corresponding to the TRT endcap regions; and $1.8 \leq |\eta| < 2$ and $2 \leq |\eta| < 2.5$, corresponding to the TRT endcap edge.

The $J/\psi \to \mu^+\mu^-$ yields are extracted from individual mass fits in each ($|\eta_1|$, $|\eta_2|$) bin, separately for events satisfying the supporting trigger and for events satisfying both the supporting and L1 TRT triggers. The resulting yields are then used to calculate the L1 TRT trigger efficiencies. These are then compared with the efficiencies calculated similarly in signal MC to derive per-event trigger efficiency scale factors (SFs). Figure 6 shows the measured L1 TRT trigger efficiencies and SFs for dimuon events as a function of $|\eta_1|$ and $|\eta_2|$. The observed efficiency is around 60–90% if at least one muon is found in the TRT barrel region, and is approximately 80–90% if at least one muon is in the TRT endcap region. The efficiency drops typically to 14–50% if there is a muon in either transition or TRT endcap edge regions. Similarly, the extracted SF values vary with $|\eta_1|$ and $|\eta_2|$, as seen in figure 6(b). The mismodeling of the L1 TRT trigger efficiency in MC simulation observed in figure 6(b) is due to the TRT module-level deadtime that is not accounted for in the simulation.

The measured SFs are used to correct the simulated signal and background MC events. They are applied as multiplicative factors to the MC event weights. In particular, they improve the ϵ_C factors used in eq. (6.1) by providing an accurate description of the L1 TRT trigger efficiency as a function of y. Due to the limited size of the data sample from the supporting trigger, the same SFs (as derived for muon pairs) are applied also to the dielectron final states. Possible differences between the SFs for muons and electrons are

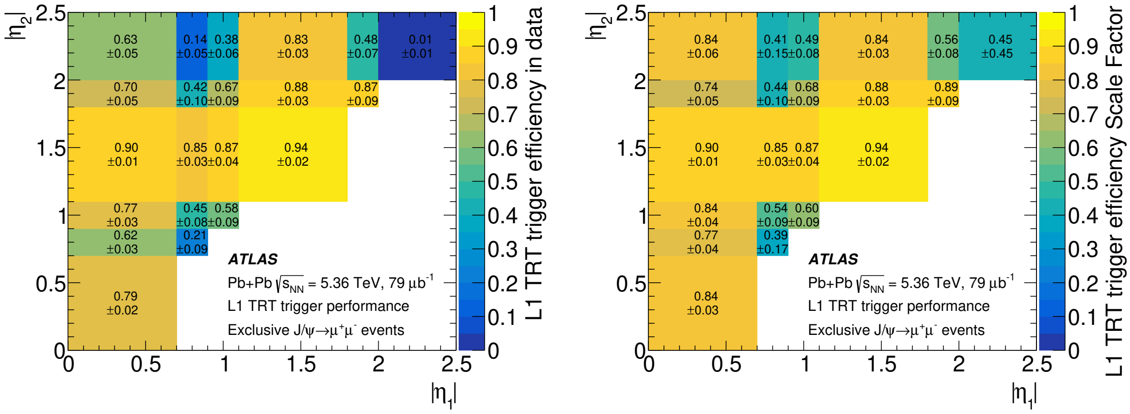

(a) (b)

Figure 6. L1 TRT trigger (a) efficiency and (b) scale factors for dimuon events in data as a function of $|\eta_1|$ and $|\eta_2|$. Numerical values of trigger efficiency and scale factors are also shown, along with the respective statistical uncertainties.

taken into account in the signal mass fit procedure (section 5.3), by allowing the relative yields of $J/\psi \to e^+e^-$ and $J/\psi \to \mu^+\mu^-$ events to float. No dependence of the L1 TRT trigger SFs on other aspects of the muon-pair kinematics, including the individual p_{T} of the muons, is observed. Similarly, the muon charge and azimuthal angle efficiency-dependence is well modelled in the MC simulation.

The HLT selection efficiency of the signal trigger is studied using exclusive 2-track events satisfying the supporting trigger with the same L1 selection as the signal trigger, but with relaxed HLT requirements. The same event selection as the SR is also used. The HLT selection efficiency in data is found to be above 99% for the signal process. Good agreement is found between the HLT efficiency in data and in MC simulation, and thus no additional HLT correction is applied to MC-simulated events.

8 Systematic uncertainties

Systematic uncertainties in the coherent J/ψ cross section measurements arise from the reconstruction of ID tracks, the trigger efficiency estimation, signal and background modeling, the integrated luminosity uncertainty, and the $J/\psi \to \mu^+\mu^-$ branching fraction uncertainty.

8.1 Detector material modeling

For evaluating the systematic uncertainties of the ID material description, alternative MC-simulated signal and background samples are produced. These implement variations in the amount of material in different ID regions used in the detector simulation: the passive material of the ID is scaled up by 5%, the passive material of the innermost ID layer is scaled up by 10%, or the passive material in the services region is scaled up by 25%. These variations capture the full range of data-MC differences observed in studies of the ID material [46]. The impact of these variations on the analysis can be two-fold: a change in the signal efficiency due to changes in track reconstruction efficiency, and changes in the shape of the $m_{\mu^+\mu^-}$ distribution

Absolute rapidity interval	0–0.5	0.5–1	1–1.5	1.5–2	2–2.5
$J/\psi \to \mu^+\mu^-$ $m_{\mu^+\mu^-}$ lineshape	1.4%	1.2%	0.7%	0.7%	0.6%
$J/\psi \to e^+e^-$ $m_{\mu^+\mu^-}$ lineshape	0.7%	0.6%	0.3%	0.2%	0.1%
$p_{\mathrm{T}}^{\mu^+\mu^-}$ shape	0.1%	0.1%	0.1%	0.2%	0.3%
Total ID material unc. on signal yield	2.1%	1.8%	0.9%	1.0%	0.8%

Table 2. Systematic uncertainty in the measured coherent $J/\psi \to \mu^+\mu^-$ yields due to the impact of variations in detector geometry description on $m_{\mu^+\mu^-}$ and $p_{\mathrm{T}}^{\mu^+\mu^-}$ template shapes. The last row shows the total uncertainty accounting for a correlated variation of all template shapes.

($m_{\mu^+\mu^-}$ lineshape). The differences between the nominal signal yield and the one measured using each material variation is taken as systematic uncertainty. Then the symmetrized contributions are added in quadrature to calculate the total systematic uncertainty.

The resulting variations for the signal efficiency are typically between few per mil ($0 < |y| < 2.0$) and 1.6% ($2.0 < |y| < 2.5$). The variations resulting from different template shape changes are summarized in table 2. This table shows how shape variations of individual distributions ($J/\psi \to \mu^+\mu^-$ invariant mass, $J/\psi \to e^+e^-$ invariant mass and $p_{\mathrm{T}}^{\mu^+\mu^-}$) influence the measured yields. The total uncertainty accounting for correlated variations in all three distributions is also shown. Although the electron-track momentum resolution is expected to be more sensitive to material variations than the muon-track momentum resolution, the leading contribution to the signal yield uncertainty is the $J/\psi \to \mu^+\mu^-$ mass lineshape. The shape variations of the p_{T} spectrum give negligible impact on the final results.

8.2 Trigger efficiency corrections

The statistical uncertainties in the L1 TRT trigger SFs are propagated using pseudo-experiments in which the SF values are randomly shifted according to the mean and standard deviation of the correction factor in each bin. This uncertainty affects the measured cross sections by about 1.5–2% in the $0 < |y| < 2.0$ range, and it grows to 7% in the $2.0 < |y| < 2.5$ region.

The systematic uncertainties in the L1 TRT trigger SFs are estimated by varying the selection criteria described in section 7, including tightening the $|d_0|$ requirement for each track and loosening the $p_{\mathrm{T}}^{\mu^+\mu^-}$ requirement. They are then propagated in the nominal analysis by the offset method in which the SF values are coherently shifted upwards and downwards by one standard deviation and the magnitude of the change in the measurement is computed. These variations result in an 1–3.5% change of the measured cross sections.

8.3 Signal and background modeling

The uncertainty in the signal modeling used in the signal extraction procedure ($p_{\mathrm{T}}^{\mu^+\mu^-}$ fits) is estimated by taking the full difference between the fits using the signal $p_{\mathrm{T}}^{J/\psi}$ shape reweighted to LHCb data and the signal $p_{\mathrm{T}}^{J/\psi}$ shape from STARlight. This results in 0.3–1.6% variations in the signal yield, which is taken as systematic uncertainty. The effect of the signal $p_{\mathrm{T}}^{J/\psi}$ shape uncertainty in ϵ_C and A is found to be negligible.

To evaluate the impact of the mass fit methodology assumptions, an alternative fit is performed in which no additional scaling is applied between the $J/\psi \to e^+e^-$ and $J/\psi \to \mu^+\mu^-$ components beyond what is already present in the MC simulation. The difference between this alternative and the nominal fit result is taken as an additional systematic uncertainty. The difference typically amounts to 1–3.7% as a function of y.

The uncertainties in the modeling of the $\gamma\gamma \to \ell^+\ell^-$ contribution are estimated by using, for the alternative mass shape parameterisation, a second order polynomial instead of an exponential function. This results in a 0.4–3.2% impact on the measured cross sections.

To assign an uncertainty due to the incoherent J/ψ background modeling, the $p_{\mathrm{T}}^{\mu^+\mu^-}$ fits are repeated for different fit ranges in terms of the maximum $p_{\mathrm{T}}^{\mu^+\mu^-}$ value, by varying its value between 1 GeV and 3 GeV. This typically results in a 0.2–0.3% impact on the measured cross sections.

A 20% relative uncertainty in the $\psi(2S)$ feed-down background contribution is assigned to cover data-to-simulation differences observed in the $\psi(2S)$ CR. This results in an approximately 0.5% impact on the measured cross sections.

8.4 Other systematic uncertainties

The track veto applied in the event selection could be biased by the presence of additional UPC interactions in the same or separate Pb+Pb collision, resulting in the production of extra charged particle pairs, for example from the $\gamma\gamma \to e^+e^-$ process or from the coherent $\rho^0 \to \pi^+\pi^-$ production (see section 9). To check the impact of such processes on the results, the analysis is repeated with a relaxed track veto condition, to allow events with up to four reconstructed tracks instead of exactly two. The difference between the extracted signal yield from the modified (2–4 tracks) and nominal (exactly two tracks) track-veto requirements is taken as a systematic uncertainty. This difference is 2.1% with no dependence on y.

To cross-check event activity in the SR beyond the ID acceptance ($|\eta| < 2.5$), topological clusters of calorimeter-cell energy deposits [52] are studied. These topoclusters, calibrated to account for noise suppression, are required to have transverse energy $E_{\mathrm{T}} > 0.2$ GeV and pseudorapidity in the range of $3.1 < |\eta| < 4.9$. Additionally, they must satisfy the cell significance criteria for the measured energy, as outlined in ref. [53], to suppress contributions from electronic noise fluctuations. Approximately 4% of events in the SR contain at least one additional topocluster. This observation is consistent with expectations from incoherent backgrounds and the production of extra particle pairs in the forward region for the signal process. Consequently, no additional systematic uncertainty is assigned. This cross-check also ensures that potential backgrounds with extra hadronic activity, such as those from peripheral coherent J/ψ production or from beam-gas interactions, are essentially negligible.

The uncertainty in the integrated luminosity of the data sample is 2.7%. It is derived from the calibration of the luminosity following a methodology similar to that detailed in ref. [54], using the LUCID-2 detector [55] for the baseline luminosity measurements.

The relative uncertainty in the $J/\psi \to \mu^+\mu^-$ branching ratio is 0.5% [56].

The total measurement uncertainty includes both the statistical and systematic components added in quadrature. Figure 7 shows the breakdown of the uncertainties for the differential cross section measurement. The total measurement uncertainty is around 5–6%,

JHEP04(2026)020

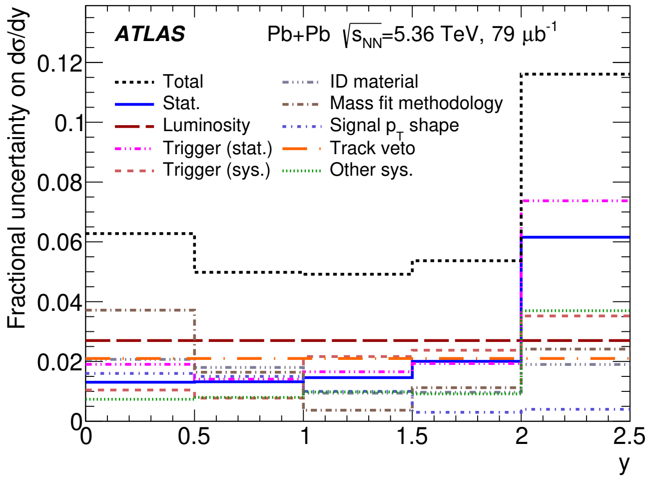

Figure 7. Breakdown of the individual uncertainty contributions as a function of y. The total measurement uncertainty, calculated by adding all contributions in quadrature, is also shown.

except the last rapidity bin where the statistical uncertainty and the trigger scale factor statistical uncertainties are larger.

9 Results

The coherent exclusive J/ψ meson differential cross sections extrapolated to the full phase space are obtained using eq. (6.1) and include the full set of statistical and systematic uncertainties. The measured differential cross sections are shown in figure 8(a). Measured cross section values are compared with predictions from STARlight (using classical Glauber option) and two calculations based on the color glass condensate (CGC) approach, one of which also includes the effect of nucleon shape fluctuations [7, 57]. Both STARlight and CGC models use HERA $\gamma p \to J/\psi p$ data as an input. Predictions from other theoretical calculations are also shown in figure 8(a) for comparison. The color dipole (CD) models [17], with different parameterizations (labeled BGK, GBW, and IIM), assume quark-antiquark dipole scattering off the nuclear target. The leading-twist approximation (LTA) [58] is a perturbative QCD calculation that accounts for nuclear shadowing effects arising from multi-nucleon interference. Both weak and strong shadowing scenarios are shown. Among the models considered, the color dipole calculations provide the best description of the data. The data also agree with NLO perturbative QCD calculations from ref. [19] (not shown in figure 8(a)), albeit within large scale uncertainties.

To quantify the level of nuclear suppression observed at mid-rapidity, the results obtained for $|y| < 0.5$ are compared with the impulse approximation (IA) model [59] as implemented in STARlight. This model is based on a simple scaling of the experimental data from exclusive J/ψ photoproduction off protons, includes the nuclear form factor, and neglects all other nuclear effects except for coherence. The ratio of the measured cross section to the IA model prediction is found to be $S^2_{\mathrm{Pb}}(|y| < 0.5) = 0.57 \pm 0.04$, indicating significant nuclear suppression.

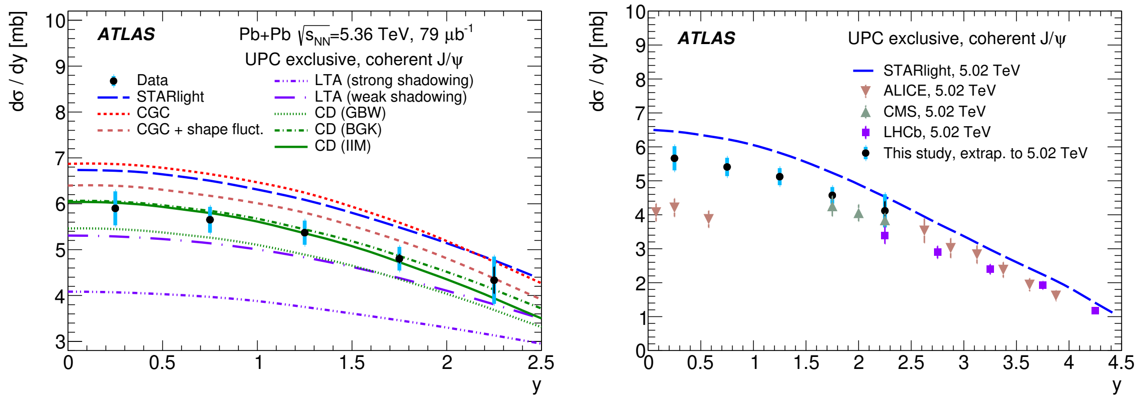

(a) (b)

Figure 8. (a) Measured differential cross section for coherent exclusive J/ψ meson production in Pb+Pb UPC at $\sqrt{s_{\mathrm{NN}}} = 5.36\,\mathrm{TeV}$ as a function of J/ψ rapidity (averaged over both sides). Data (points) are compared with several model predictions: STARlight 2.0 (using classical Glauber option), two versions of a color glass condensate (CGC) model [7, 57], color dipole (CD) models (BGK, GBW and IIM) [17], and leading-twist approximation (LTA) weak and strong shadowing models [58]. For each measurement, the thin vertical bar represents the statistical uncertainty, and the thick bar represents the total uncertainty (with statistical and systematic uncertainties added in quadrature). (b) Measured differential cross section for coherent J/ψ meson production in Pb+Pb UPC at $\sqrt{s_{\mathrm{NN}}} = 5.02\,\mathrm{TeV}$ as a function of J/ψ rapidity. The plot displays the previous results from the ALICE [25, 26], CMS [28] and LHCb [30] experiments, together with the results presented here after extrapolation to 5.02 TeV. Data (points) are compared with STARlight predictions.

To compare this measurement with previous measurements from the ALICE, CMS and LHCb Collaborations at $\sqrt{s_{\mathrm{NN}}} = 5.02\,\mathrm{TeV}$, the measured cross sections need to be extrapolated from 5.36 TeV to 5.02 TeV. The extrapolation factor is estimated by using STARlight and is found to reduce the cross sections by 4–5%, depending on the rapidity.[3] Figure 8(b) presents the results from the ALICE [25, 26], CMS [28] and LHCb [30] experiments, together with the results presented here, after extrapolation to 5.02 TeV. While the extrapolated measurement matches quite well (within 1–1.5 standard deviation) previously measured values at forward rapidities ($1.5 < y < 2.5$), the extrapolated results at mid-rapidity ($0 < y < 1$) differ significantly from the existing ALICE measurements [26].

A significant difference between the extrapolated measurement and the previous ALICE result may be due to the production of additional particle pairs accompanying the produced J/ψ meson, which are rejected by selections on the ALICE forward counters [26]. The production rate of these extra particle pairs is dominated by soft e^+e^- pair production. However, at higher pair invariant masses, the production of $\mu^+\mu^-$ pairs and $\pi^+\pi^-$ pairs from coherent ρ^0 decays is also possible [60, 61]. For the measurements of exclusive processes, these extra pairs may violate the exclusivity requirements, as suggested in ref. [62], and induce the rejection of signal events. As shown in section 8.4, this measurement has little sensitivity to

[3] A similar extrapolation factor, of the order of 4–5%, is obtained when using the CGC-based and CD-based models.

JHEP04(2026)020

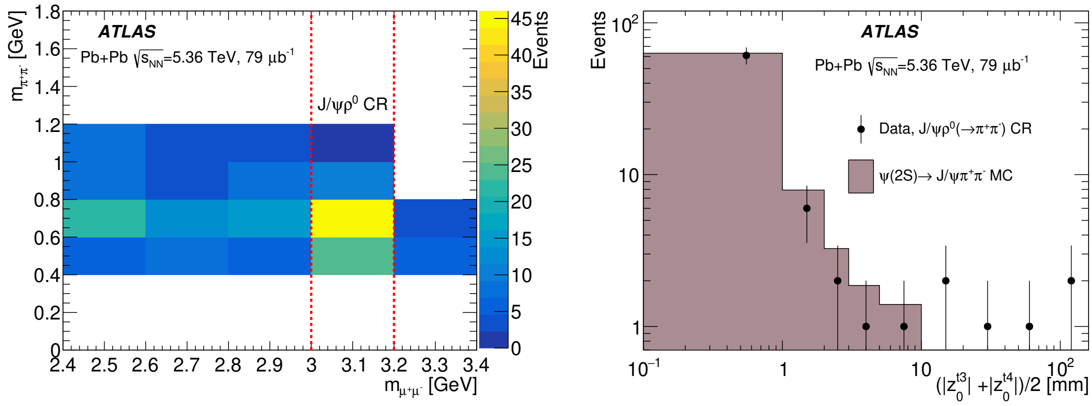

(a) (b)

Figure 9. (a) Correlation between the invariant mass of the two leading tracks and the invariant mass of the two sub-leading tracks for events satisfying $J/\psi\rho^0$ selection, after relaxing the $3 < m_{\mu^+\mu^-} < 3.2\,\text{GeV}$ requirement. The boundaries at $m_{\pi^+\pi^-} = 0.4\,\text{GeV}$ and $m_{\pi^+\pi^-} = 1.2\,\text{GeV}$ are due to selection requirements correlated with $m_{\pi^+\pi^-}$. (b) Average longitudinal impact parameter distribution of the third and fourth leading track for the $J/\psi\rho^0$ selected events in data (points). The distribution is compared with simulated $\psi(2\text{S}) \to J/\psi(\to \ell^+\ell^-)\pi^+\pi^-$ MC events.

additional particles created in the same UPC collision, presumably due to the extra particles being typically emitted outside the η and p_T acceptance of the ID.

Although ATLAS cannot study forward e^+e^- production associated with the J/ψ, primarily due its limited acceptance in high pseudorapidity region for low energy electrons, a related check has been performed using the $J/\psi(\to \ell^+\ell^-)\rho^0(\to \pi^+\pi^-)$ process. For example, the relative rate of coincident production of J/ψ and ρ^0, compared with those from separate collisions, can be checked. Figure 9(a) presents the correlation between $m_{\mu^+\mu^-}$ and $m_{\pi^+\pi^-}$ for events satisfying the $J/\psi\rho^0$ control region selections summarized in section 5.1, where a clear simultaneous $J/\psi\rho^0$ contribution is visible. Because the ρ^0 is a broad resonance, no further selection is applied to the $m_{\pi^+\pi^-}$ spectrum.

To study the contributions of $J/\psi\rho^0$ events coming from the same or separate Pb+Pb collisions, it is examined whether the two particle pairs come from the same vertex or from different ones. Since the low p_T of the ρ^0 decay tracks often leads to no vertex being reconstructed, this is done by checking the probability of the ρ^0 tracks to have a large longitudinal impact parameter relative to the reconstructed J/ψ vertex, $|z_0| > 2$ mm. Figure 9(b) shows the average longitudinal impact parameter distribution of the third and fourth leading track from the $J/\psi\rho^0$ selection in data. A low-lying tail is observed in this distribution at large average longitudinal impact parameter values, indicating simultaneous $J/\psi\rho^0$ production from separate Pb+Pb interactions. This distribution is compared with the same distribution from simulated $\psi(2\text{S}) \to J/\psi(\to \ell^+\ell^-)\pi^+\pi^-$ MC events, to check the expected shape from the single Pb+Pb interaction events: the two processes clearly arise from the same vertex at a much higher rate than for separate ones. A similar process that shares similar topology, $\gamma\gamma \to \mu^+\mu^- + \rho^0$, has recently been measured by ATLAS [63], highlighting the importance of these effects. Further studies will be needed to assess the

JHEP04(2026)020

relative impact of these processes on the event selection requirements used by the different experiments. Notably, the relative rates for $J/\psi + e^+e^-$ production from a single interaction over separate interactions can differ substantially from those from $J/\psi\rho^0$ due to differences between the kinematics of the respective processes.

10 Conclusions

A first measurement of coherent exclusive J/ψ production in ultraperipheral collisions in ATLAS is presented. The measurement uses 79 μb^{-1} of Pb+Pb collision data recorded at the LHC in 2023 at $\sqrt{s_{\mathrm{NN}}} = 5.36$ TeV. Events were selected with a special Level 1 trigger only requiring a signal in the ATLAS transition radiation tracking detector. Results are corrected for all known backgrounds to the dimuon decay channel, with the $J/\psi \to e^+e^-$ channel subtracted as a background due to distortions to the mass peak and reconstruction efficiency from detector material effects. Differential cross sections are measured as a function of J/ψ rapidity in the rapidity interval $|y| < 2.5$ and are compared with theory predictions and, after extrapolation to $\sqrt{s_{\mathrm{NN}}} = 5.02$ TeV, with previous measurements from other LHC experiments. The data are best described by calculations based on the color dipole model. Significant tension is observed with ALICE data at mid-rapidity when extrapolating this measurement to 5.02 TeV. This tension may be related to the effect of additional UPC processes, from the same Pb+Pb interaction, on the signal exclusivity conditions.

Acknowledgments

We thank CERN for the very successful operation of the LHC and its injectors, as well as the support staff at CERN and at our institutions worldwide without whom ATLAS could not be operated efficiently.

The crucial computing support from all WLCG partners is acknowledged gratefully, in particular from CERN, the ATLAS Tier-1 facilities at TRIUMF/SFU (Canada), NDGF (Denmark, Norway, Sweden), CC-IN2P3 (France), KIT/GridKA (Germany), INFN-CNAF (Italy), NL-T1 (Netherlands), PIC (Spain), RAL (U.K.) and BNL (U.S.A.), the Tier-2 facilities worldwide and large non-WLCG resource providers. Major contributors of computing resources are listed in ref. [64].

We gratefully acknowledge the support of ANPCyT, Argentina; YerPhI, Armenia; ARC, Australia; BMWFW and FWF, Austria; ANAS, Azerbaijan; CNPq and FAPESP, Brazil; NSERC, NRC and CFI, Canada; CERN; ANID, Chile; CAS, MOST and NSFC, China; Minciencias, Colombia; MEYS CR, Czech Republic; DNRF and DNSRC, Denmark; IN2P3-CNRS and CEA-DRF/IRFU, France; SRNSFG, Georgia; BMFTR, HGF and MPG, Germany; GSRI, Greece; RGC and Hong Kong SAR, China; ICHEP and Academy of Sciences and Humanities, Israel; INFN, Italy; MEXT and JSPS, Japan; CNRST, Morocco; NWO, Netherlands; RCN, Norway; MNiSW, Poland; FCT, Portugal; MNE/IFA, Romania; MSTDI, Serbia; MSSR, Slovakia; ARIS and MVZI, Slovenia; DSI/NRF, South Africa; MICIU/AEI, Spain; SRC and Wallenberg Foundation, Sweden; SERI, SNSF and Cantons of Bern and Geneva, Switzerland; NSTC, Taipei; TENMAK, Türkiye; STFC/UKRI, United Kingdom; DOE and NSF, United States of America.

JHEP04(2026)020

Individual groups and members have received support from BCKDF, CANARIE, CRC and DRAC, Canada; CERN-CZ, FORTE and PRIMUS, Czech Republic; COST, ERC, ERDF, Horizon 2020, ICSC-NextGenerationEU and Marie Skłodowska-Curie Actions, European Union; Investissements d'Avenir Labex, Investissements d'Avenir Idex and ANR, France; DFG and AvH Foundation, Germany; Herakleitos, Thales and Aristeia programmes co-financed by EU-ESF and the Greek NSRF, Greece; BSF-NSF and MINERVA, Israel; NCN and NAWA, Poland; La Caixa Banking Foundation, CERCA Programme Generalitat de Catalunya and PROMETEO and GenT Programmes Generalitat Valenciana, Spain; Göran Gustafssons Stiftelse, Sweden; The Royal Society and Leverhulme Trust, United Kingdom; United States of America.

In addition, individual members wish to acknowledge support from CERN: European Organization for Nuclear Research (CERN DOCT); Chile: Agencia Nacional de Investigación y Desarrollo (ANID FONDECYT reg. 1230987, FONDECYT 1230812, FONDECYT 1240864, Fondecyt 3240661, Fondecyt Regular 1240721); China: Chinese Ministry of Science and Technology (MOST-2023YFA1605700, MOST-2023YFA1609300), National Natural Science Foundation of China (NSFC – 12175119, NSFC 12275265); Czech Republic: Czech Science Foundation (GACR – 24-11373S), Ministry of Education Youth and Sports (ERC-CZ-LL2327, FORTE CZ.02.01.01/00/22_008/0004632), PRIMUS Research Programme (PRIMUS/21/SCI/017); EU: H2020 European Research Council (ERC – 101002463); European Union: European Research Council (BARD No. 101116429, ERC – 948254, ERC 101089007), European Regional Development Fund (HE COFUND GA No.101081355, ERDF), European Union, Future Artificial Intelligence Research (FAIR-NextGenerationEU PE00000013), Italian Center for High Performance Computing, Big Data and Quantum Computing (ICSC, NextGenerationEU), Marie Sklodowska-Curie Actions (GAP-101168829); France: Agence Nationale de la Recherche (ANR-21-CE31-0013, ANR-21-CE31-0022, ANR-22-EDIR-0002, ANR-24-CE31-0504-01); Germany: Baden-Württemberg Stiftung (BW Stiftung-Postdoc Eliteprogramme), Deutsche Forschungsgemeinschaft (DFG – 469666862, DFG – CR 312/5-2); China: Research Grants Council (GRF); Italy: Istituto Nazionale di Fisica Nucleare (ICSC, NextGenerationEU), Ministero dell'Università e della Ricerca (NextGenEU 153D23001490006 M4C2.1.1, NextGenEU I53D23000820006 M4C2.1.1, NextGenEU I53D23001490006 M4C2.1.1, SOE2024_0000023); Japan: Japan Society for the Promotion of Science (JSPS KAKENHI JP22H01227, JSPS KAKENHI JP22H04944, JSPS KAKENHI JP22KK0227, JSPS KAKENHI JP24K23939, JSPS KAKENHI JP24KK0251, JSPS KAKENHI JP25H00650, JSPS KAKENHI JP25H01291, JSPS KAKENHI JP25K01023); Norway: Research Council of Norway (RCN-314472); Poland: Ministry of Science and Higher Education (IDUB AGH, POB8, D4 no 9722), Polish National Science Centre (NCN 2021/42/E/ST2/00350, NCN OPUS 2023/51/B/ST2/02507, NCN OPUS nr 2022/47/B/ST2/03059, NCN UMO-2019/34/E/ST2/00393, UMO-2022/47/O/ST2/00148, UMO-2023/49/B/ST2/04085, UMO-2023/51/B/ST2/00920, UMO-2024/53/N/ST2/00869); Portugal: Foundation for Science and Technology (FCT); Spain: Agencia de Gestión de Ayudas Universitarias y de Investigación (AGAUR – 2023 BP 00141), Generalitat Valenciana (ASFAE/2022/008), Ministry of Science and Innovation (MCIN & NextGenEU PCI2022-135018-2, MICIN & FEDER PID2021-125273NB, RYC2019-028510-I, RYC2020-030254-I, RYC2021-031273-I, RYC2022-038164-I), Ministerio de Ciencia, Innovación y Universidades/Agencia Estatal de Investigación (PID2022-142604OB-C22); Sweden: Carl Trygger Foundation (Carl Trygger Foundation CTS 22:2312), Swedish Research Council (Swedish Research Council 2023-04654, VR 2021-03651, VR 2022-03845, VR 2022-04683, VR 2023-03403, VR 2024-05451), Knut and Alice Wallenberg Foundation (KAW 2018.0458, KAW 2022.0358, KAW 2023.0366); Switzerland: Swiss National Science Foundation (SNSF – PCEFP2_194658); United Kingdom: Royal Society (NIF-R1-231091); United States of America: U.S. Department of Energy (ECA DE-AC02-76SF00515), Neubauer Family Foundation.

Data Availability Statement. This article has no associated data or the data will not be deposited.

Code Availability Statement. This article has no associated code or the code will not be deposited.

References

[1] C.F. von Weizsäcker, *Radiation emitted in collisions of very fast electrons*, *Z. Phys.* **88** (1934) 612 [INSPIRE].

[2] E.J. Williams, *Nature of the high-energy particles of penetrating radiation and status of ionization and radiation formulae*, *Phys. Rev.* **45** (1934) 729 [INSPIRE].

[3] M. Harrison, T. Ludlam and S. Ozaki, *RHIC project overview*, *Nucl. Instrum. Meth. A* **499** (2003) 235 [INSPIRE].

[4] L. Evans and P. Bryant, *LHC Machine*, 2008 *JINST* **3** S08001 [INSPIRE].

[5] ATLAS collaboration, *Measurement of photonuclear jet production in ultra-peripheral Pb+Pb collisions at $\sqrt{s_{NN}} = 5.02$ TeV with the ATLAS detector*, *Phys. Rev. D* **111** (2025) 052006 [arXiv:2409.11060] [INSPIRE].

[6] A.J. Baltz, S.R. Klein and J. Nystrand, *Coherent vector meson photoproduction with nuclear breakup in relativistic heavy ion collisions*, *Phys. Rev. Lett.* **89** (2002) 012301 [nucl-th/0205031] [INSPIRE].

[7] H. Mäntysaari, F. Salazar and B. Schenke, *Nuclear geometry at high energy from exclusive vector meson production*, *Phys. Rev. D* **106** (2022) 074019 [arXiv:2207.03712] [INSPIRE].

[8] A.J. Baltz et al., *The Physics of Ultraperipheral Collisions at the LHC*, *Phys. Rept.* **458** (2008) 1 [arXiv:0706.3356] [INSPIRE].

[9] S. Klein and P. Steinberg, *Photonuclear and Two-photon Interactions at High-Energy Nuclear Colliders*, *Ann. Rev. Nucl. Part. Sci.* **70** (2020) 323 [arXiv:2005.01872] [INSPIRE].

[10] M.G. Ryskin, *Diffractive J/Ψ electroproduction in LLA QCD*, *Z. Phys. C* **57** (1993) 89 [INSPIRE].

[11] N. Armesto, *Nuclear shadowing*, *J. Phys. G* **32** (2006) R367 [hep-ph/0604108] [INSPIRE].

[12] L. Frankfurt, V. Guzey and M. Strikman, *Leading Twist Nuclear Shadowing Phenomena in Hard Processes with Nuclei*, *Phys. Rept.* **512** (2012) 255 [arXiv:1106.2091] [INSPIRE].

[13] V. Guzey, E. Kryshen, M. Strikman and M. Zhalov, *Evidence for nuclear gluon shadowing from the ALICE measurements of PbPb ultraperipheral exclusive* J/ψ *production*, *Phys. Lett. B* **726** (2013) 290 [arXiv:1305.1724] [INSPIRE].

[14] V.P. Gonçalves, B.D. Moreira and F.S. Navarra, *Investigation of diffractive photoproduction of* J/Ψ *in hadronic collisions*, *Phys. Rev. C* **90** (2014) 015203 [arXiv:1405.6977] [INSPIRE].

[15] J. Cepila, J.G. Contreras and M. Krelina, *Coherent and incoherent* J/ψ *photonuclear production in an energy-dependent hot-spot model*, *Phys. Rev. C* **97** (2018) 024901 [arXiv:1711.01855] [INSPIRE].

[16] D. Bendova, J. Cepila, J.G. Contreras and M. Matas, *Photonuclear* J/ψ *production at the LHC: Proton-based versus nuclear dipole scattering amplitudes*, *Phys. Lett. B* **817** (2021) 136306 [arXiv:2006.12980] [INSPIRE].

[17] A. Łuszczak and W. Schäfer, *Coherent photoproduction of* J/ψ *in nucleus-nucleus collisions in the color dipole approach*, *Phys. Rev. C* **99** (2019) 044905 [arXiv:1901.07989] [INSPIRE].

[18] H. Kowalski and D. Teaney, *Impact parameter dipole saturation model*, *Phys. Rev. D* **68** (2003) 114005 [hep-ph/0304189] [INSPIRE].

[19] K.J. Eskola et al., *Exclusive* J/ψ *photoproduction in ultraperipheral Pb+Pb collisions at the LHC to next-to-leading order perturbative QCD*, *Phys. Rev. C* **106** (2022) 035202 [arXiv:2203.11613] [INSPIRE].

[20] STAR collaboration, *Exclusive* J/ψ, $\psi(2s)$, *and* e^+e^- *pair production in Au+Au ultra-peripheral collisions at RHIC*, *Phys. Rev. C* **110** (2024) 014911 [arXiv:2311.13632] [INSPIRE].

[21] ALICE collaboration, *Coherent* J/ψ *photoproduction in ultra-peripheral Pb-Pb collisions at* $\sqrt{s_{NN}} = 2.76$ *TeV*, *Phys. Lett. B* **718** (2013) 1273 [arXiv:1209.3715] [INSPIRE].

[22] ALICE collaboration, *Charmonium and* e^+e^- *pair photoproduction at mid-rapidity in ultra-peripheral Pb-Pb collisions at* $\sqrt{s_{NN}} = 2.76$ *TeV*, *Eur. Phys. J. C* **73** (2013) 2617 [arXiv:1305.1467] [INSPIRE].

[23] ALICE collaboration, *Coherent* $\psi(2S)$ *photo-production in ultra-peripheral Pb Pb collisions at* $\sqrt{s}_{NN} = 2.76$ *TeV*, *Phys. Lett. B* **751** (2015) 358 [arXiv:1508.05076] [INSPIRE].

[24] CMS collaboration, *Coherent* J/ψ *photoproduction in ultra-peripheral PbPb collisions at* $\sqrt{s_{NN}} = 2.76$ *TeV with the CMS experiment*, *Phys. Lett. B* **772** (2017) 489 [arXiv:1605.06966] [INSPIRE].

[25] ALICE collaboration, *Coherent* J/ψ *photoproduction at forward rapidity in ultra-peripheral Pb-Pb collisions at* $\sqrt{s_{NN}} = 5.02$ *TeV*, *Phys. Lett. B* **798** (2019) 134926 [arXiv:1904.06272] [INSPIRE].

[26] ALICE collaboration, *Coherent* J/ψ *and* ψ' *photoproduction at midrapidity in ultra-peripheral Pb-Pb collisions at* $\sqrt{s_{NN}} = 5.02$ *TeV*, *Eur. Phys. J. C* **81** (2021) 712 [arXiv:2101.04577] [INSPIRE].

[27] ALICE collaboration, *Energy dependence of coherent photonuclear production of* J/ψ *mesons in ultra-peripheral Pb-Pb collisions at* $\sqrt{s_{NN}} = 5.02$ *TeV*, *JHEP* **10** (2023) 119 [arXiv:2305.19060] [INSPIRE].

JHEP04(2026)020

[28] CMS collaboration, *Probing Small Bjorken-x Nuclear Gluonic Structure via Coherent J/ψ Photoproduction in Ultraperipheral Pb-Pb Collisions at $\sqrt{s_{NN}} = 5.02$ TeV*, Phys. Rev. Lett. **131** (2023) 262301 [arXiv:2303.16984] [INSPIRE].

[29] LHCb collaboration, *Study of coherent J/ψ production in lead-lead collisions at $\sqrt{s_{NN}} = 5$ TeV*, JHEP **07** (2022) 117 [arXiv:2107.03223] [INSPIRE].

[30] LHCb collaboration, *Study of exclusive photoproduction of charmonium in ultra-peripheral lead-lead collisions*, JHEP **06** (2023) 146 [arXiv:2206.08221] [INSPIRE].

[31] ATLAS collaboration, *The ATLAS Experiment at the CERN Large Hadron Collider*, 2008 JINST **3** S08003 [INSPIRE].

[32] ATLAS collaboration, *The ATLAS experiment at the CERN Large Hadron Collider: a description of the detector configuration for Run 3*, 2024 JINST **19** P05063 [arXiv:2305.16623] [INSPIRE].

[33] ATLAS collaboration, *The ATLAS trigger system for LHC Run 3 and trigger performance in 2022*, 2024 JINST **19** P06029 [arXiv:2401.06630] [INSPIRE].

[34] ATLAS collaboration, *Software and computing for Run 3 of the ATLAS experiment at the LHC*, Eur. Phys. J. C **85** (2025) 234 [arXiv:2404.06335] [INSPIRE].

[35] ATLAS collaboration, *The TRT Fast-OR Trigger*, ATL-INDET-PUB-2009-002 (2009).

[36] ATLAS collaboration, *Performance of the ATLAS Transition Radiation Tracker in Run 1 of the LHC: tracker properties*, 2017 JINST **12** P05002 [arXiv:1702.06473] [INSPIRE].

[37] S.R. Klein et al., *STARlight: A Monte Carlo simulation program for ultra-peripheral collisions of relativistic ions*, Comput. Phys. Commun. **212** (2017) 258 [arXiv:1607.03838] [INSPIRE].

[38] C. Bierlich et al., *A comprehensive guide to the physics and usage of PYTHIA 8.3*, SciPost Phys. Codeb. **2022** (2022) 8 [arXiv:2203.11601] [INSPIRE].

[39] ATLAS collaboration, *Exclusive dimuon production in ultraperipheral Pb+Pb collisions at $\sqrt{s_{NN}} = 5.02$ TeV with ATLAS*, Phys. Rev. C **104** (2021) 024906 [arXiv:2011.12211] [INSPIRE].

[40] D.J. Lange, *The EvtGen particle decay simulation package*, Nucl. Instrum. Meth. A **462** (2001) 152 [INSPIRE].

[41] N. Davidson, T. Przedzinski and Z. Was, *PHOTOS interface in C++: Technical and Physics Documentation*, Comput. Phys. Commun. **199** (2016) 86 [arXiv:1011.0937] [INSPIRE].

[42] ALICE collaboration, *First polarisation measurement of coherently photoproduced J/ψ in ultra-peripheral Pb-Pb collisions at $\sqrt{s_{NN}} = 5.02$ TeV*, Phys. Lett. B **865** (2025) 139466 [arXiv:2304.10928] [INSPIRE].

[43] ALICE collaboration, *First measurement of the $|t|$-dependence of coherent J/ψ photonuclear production*, Phys. Lett. B **817** (2021) 136280 [arXiv:2101.04623] [INSPIRE].

[44] ATLAS collaboration, *Track Reconstruction Performance of the ATLAS Inner Detector at $\sqrt{s} = 13$ TeV*, ATL-PHYS-PUB-2015-018 (2015) [INSPIRE].

[45] ATLAS collaboration, *Early Inner Detector Tracking Performance in the 2015 Data at $\sqrt{s} = 13$ TeV*, ATL-PHYS-PUB-2015-051 (2015) [INSPIRE].

[46] ATLAS collaboration, *Study of the material of the ATLAS inner detector for Run 2 of the LHC*, 2017 JINST **12** P12009 [arXiv:1707.02826] [INSPIRE].

[47] ATLAS collaboration, *Performance of the ATLAS Track Reconstruction Algorithms in Dense Environments in LHC Run 2*, *Eur. Phys. J. C* **77** (2017) 673 [arXiv:1704.07983] [INSPIRE].

[48] M.J. Oreglia, *A Study of the Reactions $\psi' \to \gamma\gamma\psi$*, Appendix D, Ph.D. Thesis, SLAC-0236 (1980).

[49] CMS collaboration, *Measurement of light-by-light scattering and the Breit-Wheeler process, and search for axion-like particles in ultraperipheral PbPb collisions at $\sqrt{s_{NN}} = 5.02$ TeV*, *JHEP* **08** (2025) 006 [arXiv:2412.15413] [INSPIRE].

[50] ATLAS collaboration, *Exclusive dielectron production in ultraperipheral Pb+Pb collisions at $\sqrt{s_{NN}} = 5.02$ TeV with ATLAS*, *JHEP* **06** (2023) 182 [arXiv:2207.12781] [INSPIRE].

[51] H1 collaboration, *Elastic and proton-dissociative photoproduction of J/ψ mesons at HERA*, *Eur. Phys. J. C* **73** (2013) 2466 [arXiv:1304.5162] [INSPIRE].

[52] ATLAS collaboration, *Topological cell clustering in the ATLAS calorimeters and its performance in LHC Run 1*, *Eur. Phys. J. C* **77** (2017) 490 [arXiv:1603.02934] [INSPIRE].

[53] ATLAS collaboration, *Rapidity gap cross sections measured with the ATLAS detector in pp collisions at $\sqrt{s} = 7$ TeV*, *Eur. Phys. J. C* **72** (2012) 1926 [arXiv:1201.2808] [INSPIRE].

[54] ATLAS collaboration, *Luminosity determination in pp collisions at $\sqrt{s} = 13$ TeV using the ATLAS detector at the LHC*, *Eur. Phys. J. C* **83** (2023) 982 [arXiv:2212.09379] [INSPIRE].

[55] G. Avoni et al., *The new LUCID-2 detector for luminosity measurement and monitoring in ATLAS*, 2018 *JINST* **13** P07017 [INSPIRE].

[56] Particle Data Group collaboration, *Review of particle physics*, *Phys. Rev. D* **110** (2024) 030001 [INSPIRE].

[57] H. Mäntysaari, F. Salazar and B. Schenke, *Energy dependent nuclear suppression from gluon saturation in exclusive vector meson production*, *Phys. Rev. D* **109** (2024) L071504 [arXiv:2312.04194] [INSPIRE].

[58] V. Guzey, E. Kryshen and M. Zhalov, *Coherent photoproduction of vector mesons in ultraperipheral heavy ion collisions: Update for run 2 at the CERN Large Hadron Collider*, *Phys. Rev. C* **93** (2016) 055206 [arXiv:1602.01456] [INSPIRE].

[59] V. Guzey, M. Strikman and M. Zhalov, *Disentangling coherent and incoherent quasielastic J/ψ photoproduction on nuclei by neutron tagging in ultraperipheral ion collisions at the LHC*, *Eur. Phys. J. C* **74** (2014) 2942 [arXiv:1312.6486] [INSPIRE].

[60] S. Klein and J. Nystrand, *Exclusive vector meson production in relativistic heavy ion collisions*, *Phys. Rev. C* **60** (1999) 014903 [hep-ph/9902259] [INSPIRE].

[61] G. Baur et al., *Multi-photon exchange processes in ultraperipheral relativistic heavy ion collisions*, *Nucl. Phys. A* **729** (2003) 787 [nucl-th/0307031] [INSPIRE].

[62] L.A. Harland-Lang, V.A. Khoze and M.G. Ryskin, *Elastic photon-initiated production at the LHC: the role of hadron-hadron interactions*, *SciPost Phys.* **11** (2021) 064 [arXiv:2104.13392] [INSPIRE].

[63] ATLAS collaboration, *Measurement of coincident photon-initiated processes in ultra-peripheral Pb+Pb collisions with the ATLAS detector*, arXiv:2504.07795 [INSPIRE].

[64] ATLAS collaboration, *ATLAS Computing Acknowledgements*, ATL-SOFT-PUB-2026-001 (2026).

JHEP04(2026)020

The ATLAS collaboration

G. Aad[104], E. Aakvaag[17], B. Abbott[123], S. Abdelhameed[119a], K. Abeling[55], N.J. Abicht[49], S.H. Abidi[30], M. Aboelela[45], A. Aboulhorma[36e], H. Abramowicz[157], Y. Abulaiti[120], B.S. Acharya[69a,69b,a], A. Ackermann[63a], C. Adam Bourdarios[4], L. Adamczyk[87a], S.V. Addepalli[149], M. J. Addison[103], J. Adelman[118], A. Adiguzel[22c], T. Adye[137], A.A. Affolder[139], Y. Afik[40], M.N. Agaras[13], A. Aggarwal[102], C. Agheorghiesei[28c], F. Ahmadov[39,b], S. Ahuja[97], S. Ahuja[169], X. Ai[143b], G. Aielli[76a,76b], A. Aikot[169], M. Ait Tamlihat[36e], B. Aitbenchikh[36a], M. Akbiyik[102], T.P.A. Åkesson[100], A.V. Akimov[151], D. Akiyama[174], N.N. Akolkar[25], S. Aktas[172], G.L. Alberghi[24b], J. Albert[171], U. Alberti[20], P. Albicocco[53], G.L. Albouy[60], S. Alderweireldt[52], Z.L. Alegria[124], M. Aleksa[37], C. Alexa[28b], I.N. Aleksandrov[39], T. Alexopoulos[10], F. Alfonsi[24b], M. Algren[56], M. Alhroob[173], B. Ali[135], H. M. J. Ali[93,c], S. Ali[32], S.W. Alibocus[94], M. Aliev[34c], G. Alimonti[71a], W. Alkakhi[55], C. Allaire[66], B.M.M. Allbrooke[152], D. R. Allen[124], J. S. Allen[103], J.F. Allen[52], P.P. Allport[21], A. Aloisio[72a,72b], F. Alonso[92], C. Alpigiani[142], Z.M.K. Alsolami[93], A. Alvarez Fernandez[102], M. Alves Cardoso[56], M.G. Alviggi[72a,72b], M. Aly[103], A. Ambler[106], C. Amelung[37], M. Amerl[103], C.G. Ames[111], T. Amezza[130], D. Amidei[108], B. Amini[54], K. Amirie[161], A. Amirkhanov[39], S.P. Amor Dos Santos[133a], K.R. Amos[169], D. Amperiadou[158], S. An[84], C. Anastopoulos[145], T. Andeen[11], J.K. Anders[94], A. C. Anderson[59], A. Andreazza[71a,71b], S. Angelidakis[9], A. Angerami[42], A.V. Anisenkov[39], A. Annovi[74a], C. Antel[37], E. Antipov[151], M. Antonelli[53], F. Anulli[75a], M. Aoki[84], T. Aoki[159], M.A. Aparo[152], L. Aperio Bella[48], M. Apicella[31], C. Appelt[157], A. Apyan[27], M. Arampatzi[10], S. J. Arbiol Val[88], C. Arcangeletti[53], A.T.H. Arce[51], J-F. Arguin[110], S. Argyropoulos[158], J.-H. Arling[48], O. Arnaez[4], H. Arnold[151], G. Artoni[75a,75b], H. Asada[113], K. Asai[121], S. Asatryan[179], N.A. Asbah[37], R. A. Ashby Pickering[173], A. M. Aslam[97], K. Assamagan[30], R. Astalos[29a], K. S. V. Astrand[100], S. Atashi[165], R.J. Atkin[34a], H. Atmani[36f], P.A. Atmasiddha[131], K. Augsten[135], A.D. Auriol[41], V.A. Austrup[103], A.S. Avad[96], G. Avolio[37], K. Axiotis[56], A. Azzam[13], D. Babal[29b], H. Bachacou[138], K. Bachas[158,d], A. Bachiu[35], E. Bachmann[50], M. J. Backes[63a], A. Badea[40], T.M. Baer[108], P. Bagnaia[75a,75b], M. Bahmani[19], D. Bahner[54], K. Bai[126], J.T. Baines[137], L. Baines[96], O.K. Baker[178], E. Bakos[16], D. Bakshi Gupta[8], L.E. Balabram Filho[83b], V. Balakrishnan[123], R. Balasubramanian[4], E.M. Baldin[38], P. Balek[87a], E. Ballabene[24b,24a], F. Balli[138], L.M. Baltes[63a], W.K. Balunas[33], J. Balz[102], I. Bamwidhi[119b], E. Banas[88], M. Bandieramonte[132], A. Bandyopadhyay[25], S. Bansal[25], L. Barak[157], M. Barakat[48], E.L. Barberio[107], D. Barberis[18b], M. Barbero[104], M. Z. Barel[117], T. Barillari[112], M-S. Barisits[37], T. Barklow[149], P. Baron[136], D.A. Baron Moreno[103], A. Baroncelli[62], A.J. Barr[129], J.D. Barr[98], F. Barreiro[101], J. Barreiro Guimarães da Costa[14], M.G. Barros Teixeira[133a], R.F. Coelho Barrue[133a], S. Barsov[38], F. Bartels[63a], R. Bartoldus[149], A.E. Barton[93], P. Bartos[29a], M. Baselga[49], S. Bashiri[88], A. Bassalat[66,e], M.J. Basso[162a], S. Bataju[45], R. Bate[170], R.L. Bates[59], S. Batlamous[101], M. Battaglia[139], D. Battulga[19], M. Bauce[75a,75b], M. Bauer[79], P. Bauer[25], L. T. Bayer[48], L.T. Bazzano Hurrell[31], J.B. Beacham[112], T. Beau[130], J.Y. Beaucamp[92], P.H. Beauchemin[164], P. Bechtle[25], H.P. Beck[20,f], K. Becker[173], A.J. Beddall[82],

JHEP04(2026)020

V.A. Bednyakov[39], C.P. Bee[151], L.J. Beemster[16], M. Begalli[83d], M. Begel[30], J.K. Behr[48], J.F. Beirer[37], F. Beisiegel[25], M. Belfkir[119b], G. Bella[157], L. Bellagamba[24b], A. Bellerive[35], C.D. Bellgraph[68], P. Bellos[21], K. Beloborodov[38], I. Benaoumeur[21], D. Benchekroun[36a], F. Bendebba[36a], Y. Benhammou[157], K.C. Benkendorfer[61], L. Beresford[48], M. Beretta[53], E. Bergeaas Kuutmann[167], N. Berger[4], B. Bergmann[135], J. Beringer[18a], G. Bernardi[5], C. Bernius[149], F.U. Bernlochner[25], A. Berrocal Guardia[13], T. Berry[97], P. Berta[136], A. Berthold[50], A. Berti[133a], R. Bertrand[104], S. Bethke[112], A. Betti[75a,75b], A.J. Bevan[96], L. Bezio[56], N.K. Bhalla[54], S. Bharthuar[112], S. Bhatta[151], P. Bhattarai[149], Z.M. Bhatti[120], K. D. Bhide[54], V.S. Bhopatkar[124], R.M. Bianchi[132], G. Bianco[24b,24a], O. Biebel[111], M. Biglietti[77a], C. S. Billingsley[45], Y. Bimgdi[36f], M. Bindi[55], A. Bingham[177], A. Bingul[22b], C. Bini[75a,75b], G.A. Bird[33], M. Birman[175], M. Biros[136], S. Biryukov[152], T. Bisanz[49], E. Bisceglie[24b,24a], J.P. Biswal[137], D. Biswas[147], I. Bloch[48], A. Blue[59], U. Blumenschein[96], V.S. Bobrovnikov[39], L. Boccardo[57b,57a], M. Boehler[54], D. Bogavac[13], A.G. Bogdanchikov[38], L. S. Boggia[130], B. Boehm[172], V. Boisvert[97], P. Bokan[37], T. Bold[87a], M. Bomben[5], M. Bona[96], M. Boonekamp[138], A.G. Borbély[59], I.S. Bordulev[38], G. Borissov[93], D. Bortoletto[129], D. Boscherini[24b], K. Bouaouda[36a], N. Bouchhar[169], L. Boudet[4], J. Boudreau[132], E.V. Bouhova-Thacker[93], D. Boumediene[41], R. Bouquet[57b,57a], A. Boveia[122], J. Boyd[37], D. Boye[30], I.R. Boyko[39], L. Bozianu[56], J. Bracinik[21], N. Brahimi[4], G. Brandt[177], O. Brandt[33], B. Brau[105], J.E. Brau[126], L. Brenner[117], R. Brenner[167], S. Bressler[175], G. Brianti[78a,78b], D. Britton[59], D. Britzger[112], I. Brock[25], R. Brock[109], G. Brooijmans[42], A.J. Brooks[68], E. M. Brooks[162b], E. Brost[30], L.M. Brown[171,162a], L.E. Bruce[61], T.L. Bruckler[129], P.A. Bruckman de Renstrom[88], B. Brüers[48], A. Bruni[24b], G. Bruni[24b], D. Brunner[47a,47b], M. Bruschi[24b], N. Bruscino[75a,75b], T. Buanes[17], Q. Buat[142], D. Buchin[112], A.G. Buckley[59], V. Büscher[102], O. Bulekov[82], B.A. Bullard[149], S. Burdin[94], C.D. Burgard[49], A.M. Burger[91], B. Burghgrave[8], O. Burlayenko[54], J. Burleson[168], J.C. Burzynski[148], E.L. Busch[42], P.J. Bussey[59], O. But[25], J.M. Butler[26], C.M. Buttar[59], J.M. Butterworth[98], W. Buttinger[137], C.J. Buxo Vazquez[109], A.R. Buzykaev[39], S. Cabrera Urbán[169], L. Cadamuro[66], H. Cai[37], Y. Cai[24b,114c,24a], Y. Cai[114a], V.M.M. Cairo[37], O. Cakir[3a], N. Calace[37], P. Calafiura[18a], G. Calderini[130], P. Calfayan[35], L. Calic[100], G. Callea[59], L.P. Caloba[83b], D. Calvet[41], S. Calvet[41], R. Camacho Toro[130], S. Camarda[37], D. Camarero Munoz[27], P. Camarri[76a,76b], C. Camincher[171], M. Campanelli[98], A. Camplani[43], V. Canale[72a,72b], A.C. Canbay[3a], E. Canonero[97], J. Cantero[169], Y. Cao[168], F. Capocasa[27], M. Capua[44b,44a], A. Carbone[71a,71b], R. Cardarelli[76a], J.C.J. Cardenas[8], M. P. Cardiff[27], J.M. Silva[52], G. Carducci[44b,44a], T. Carli[37], G. Carlino[72a], J.I. Carlotto[13], B.T. Carlson[132,g], E.M. Carlson[171], J. Carmignani[94], L. Carminati[71a,71b], A. Carnelli[4], M. Carnesale[37], S. Caron[116], E. Carquin[140g], I.B. Carr[107], S. Carrá[73a,73b], G. Carratta[24b,24a], C. Carrion Martinez[169], A.M. Carroll[126], M.P. Casado[13,h], P. Casolaro[72a,72b], M. Caspar[48], W.R. Castiglioni[40], F.L. Castillo[4], L. Castillo Garcia[13], V. Castillo Gimenez[169], N.F. Castro[133a,133e], M.C.N. Fiolhais[133a,133c,i], A. Catinaccio[37], J.R. Catmore[128], T. Cavaliere[4], V. Cavaliere[30], L.J. Caviedes Betancourt[23b], E. Celebi[82], S. Cella[37], V. Cepaitis[56], K. Cerny[125], A. Cerri[74a,j], L. Cerrito[76a,76b], F. Cerutti[18a],

JHEP04(2026)020

B. Cervato[71a,71b], A. Cervelli[24b], G. Cesarini[53], S.A. Cetin[82], P.M. Chabrillat[130], R. Chakkappai[66], S. Chakraborty[173], A. Chambers[61], J. Chan[18a], W.Y. Chan[159], J.D. Chapman[33], E. Chapon[138], B. Chargeishvili[155b], D.G. Charlton[21], C. Chauhan[136], Y. Che[114a], S. Chekanov[6], B. Chen[157], B. Chen[171], H. Chen[114a], H. Chen[30], J. Chen[144a], J. Chen[148], M. Chen[129], S. Chen[89], S.J. Chen[114a], X. Chen[144a], X. Chen[15,k], Z. Chen[62], C.L. Cheng[176], H.C. Cheng[64a], S. Cheong[149], A. Cheplakov[39], E. Cherepanova[117], R. Cherkaoui El Moursli[36e], E. Cheu[7], K. Cheung[65], L. Chevalier[138], V. Chiarella[53], G. Chiarelli[74a], G. Chiodini[70a], A.S. Chisholm[21], A. Chitan[28b], M. Chitishvili[169], M.V. Chizhov[39,l], K. Choi[11], Y. Chou[142], E.Y.S. Chow[116], V.A. Schegelsky[38], K.L. Chu[175], M.C. Chu[64a], X. Chu[14,114c], Z. Chubinidze[53], J. Chudoba[134], J.J. Chwastowski[88], D. Cieri[112], K.M. Ciesla[87a], V. Cindro[95], A. Ciocio[18a], F. Cirotto[72a,72b], Z.H. Citron[175], M. Citterio[71a], D.A. Ciubotaru[28b], A. Clark[56], P.J. Clark[52], N. Clarke Hall[98], C. Clarry[161], S.E. Clawson[48], C. Clement[47a,47b], L. Clissa[24b,24a], Y. Coadou[104], M. Cobal[69a,69c], A. Coccaro[57b], R. Coelho Lopes De Sa[105], S. Coelli[71a], L. S. Colangeli[161], B. Cole[42], P. Collado Soto[101], J. Collot[60], M.R. Coluccia[70a], P. Conde Muiño[133a,133g], M.P. Connell[34c], S.H. Connell[34c], E.I. Conroy[129], M. Contreras Cossio[11], F. Conventi[72a,m], L. Corazzina[75a,75b], F. A. Corchia[24b,24a], A. Cordeiro Oudot Choi[142], L.D. Corpe[41], M. Corradi[75a,75b], F. Corriveau[106,n], A. Cortes-Gonzalez[159], M.J. Costa[169], F. Costanza[4], D. Costanzo[145], J. Couthures[4], G. Cowan[97], K. Cranmer[176], L. Cremer[49], D. Cremonini[24b,24a], S. Crépé-Renaudin[60], F. Crescioli[130], T. Cresta[73a,73b], M. Cristinziani[147], M. Cristoforetti[78a,78b], E. Critelli[98], V. Croft[117], G. Crosetti[44b,44a], A. Cueto[101], H. Cui[98], Z. Cui[7], B.M. Cunnett[152], W.R. Cunningham[59], F. Curcio[169], J. R. Curran[52], G. D'amen[30], V. D'Amico[111], M. D'Andrea[57b,57a], G. D'anniballe[74a,74b], S. D'Auria[71a,71b], A. D'Avanzo[72a,72b], L. D'Eramo[41], A. D'Onofrio[72a,72b], M. D'Onofrio[94], M. D'uffizi[103], J.V. Da Fonseca Pinto[83b], A. Gomes[133a,133b], C. Da Via[103], W. Dabrowski[87a], T. Dado[37], S. Dahbi[154], T. Dai[108], D. Dal Santo[20], C. Dallapiccola[105], M. Dam[43], J.R. Dandoy[35], D. Dannheim[37], M. Danninger[148], V. Dao[151], G. Darbo[57b], S.J. Das[30], F. Dattola[48], T. Davidek[136], J. Davidson[173], I. Dawson[96], K. De[8], F.A. Dias[117], C. De Almeida Rossi[161], R. De Asmundis[72a], N. De Biase[48], S. De Castro[24b,24a], N. De Groot[116], P. de Jong[117], H. De la Torre[118], A. De Maria[114a], A. De Salvo[75a], U. De Sanctis[76a,76b], F. De Santis[70a,70b], A. De Santo[152], J.B. De Vivie De Regie[60], J. Debevc[95], D.V. Dedovich[39], J. Degens[94], A.M. Deiana[45], J. Del Peso[101], L. Delagrange[130], F. Deliot[138], C.M. Delitzsch[49], A. Dell'Acqua[37], L. Dell'Asta[71a,71b], M. Della Pietra[72a,72b], D. Della Volpe[56], M. Delmastro[4], C.C. Delogu[102], P.A. Delsart[60], S. Demers[178], M. Demichev[39], S.P. Denisov[38], H. Denizli[22a,o], D. Derendarz[88], F. Derue[130], P. Dervan[94,†], A. M. Desai[1], K. Desch[25], F.A. Di Bello[57b,57a], A. Di Ciaccio[76a,76b], L. Di Ciaccio[4], A. Di Domenico[75a,75b], C. Di Donato[72a,72b], A. Di Girolamo[37], G. Di Gregorio[62], A. Di Luca[78a,78b], B. Di Micco[77a,77b], R. Di Nardo[77a,77b], K.F. Di Petrillo[40], M. Diamantopoulou[35], M.A. Diaz[140a,140b], A. R. Didenko[39], M. Didenko[169], S.D. Diefenbacher[18a], E.B. Diehl[108], S. Díez Cornell[48], C. Diez Pardos[147], C. Dimitriadi[150], A. Dimitrievska[21], A. Dimri[151], Y. Ding[62], J. Dingfelder[25], T. Dingley[129], I-M. Dinu[28b], S.J. Dittmeier[63b], F. Dittus[37],

M. Divisek[136], B. Dixit[94], F. Djama[104], T. Djobava[155b], Y. Amaral Coutinho[83b], C. Doglioni[103,100], A. Dohnalova[29a], Z. Dolezal[136], K. Domijan[87a], K.M. Dona[40], M. Donadelli[83d], B. Dong[109], D. Qichen[129], J. Donini[41], J. Dopke[137], A. Doria[72a], N. Dos Santos Fernandes[133a], I.A. Dos Santos Luz[83e], P. Dougan[103], M.T. Dova[92], A.T. Doyle[59], M.P. Drescher[55], E. Dreyer[175], I. Drivas-koulouris[10], M. Drnevich[120], D. Du[62], T.A. du Pree[117], Z. Duan[114a], M. Dubau[4], F. Dubinin[39], M. Dubovsky[29a], E. Duchovni[175], G. Duckeck[111], P. K. Duckett[98], O.A. Ducu[28b], D. Duda[52], A. Dudarev[37], M.M. Dudek[88], E. R. Duden[27], M. Dührssen[37], L. Duflot[66], I. Duminica[28g], A.E. Dumitriu[28b], M. Dunford[63a], K. Dunne[47a,47b], A. Duperrin[104], A. Durglishvili[155b], G.I. Dyckes[18a], M. Dyndal[87a], B.S. Dziedzic[37], Z.O. Earnshaw[152], G.H. Eberwein[129], B. Eckerova[29a], S. Eggebrecht[55], G. Eigen[17], K. Einsweiler[18a], T. Ekelof[167], P.A. Ekman[100], S. El Farkh[36b], Y. El Ghazali[62], H. El Jarrari[34j], A. El Moussaouy[36a], D. Elitez[37], M. Ellert[167], F. Ellinghaus[177], T.A. Elliot[97], N. Ellis[37], J. Elmsheuser[30], M. Elsawy[119a], M. Elsing[37], D. Emeliyanov[137], Y. Enari[84], S. Epari[110], D. Ernani Martins Neto[88], F. Ernst[37], M. Escalier[66], C. Escobar[169], E. Etzion[157], H. Evans[68], L.S. Evans[48], A. Ezhilov[38], S. Ezzarqtouni[36a], F. Fabbri[24b,24a], L. Fabbri[24b,24a], G. Facini[98], V. Fadeyev[139], R.M. Fakhrutdinov[38], D. Fakoudis[102], S. Falciano[75a], L.F. Falda Ulhoa Coelho[133a], F. Fallavollita[112], G. Falsetti[44b,44a], J. Faltova[136], C. Fan[168], K. Y. Fan[64b], Y. Fan[14], Y. Fang[14,114c], M. Fanti[71a,71b], M. Faraj[69a,69b], Z. Farazpay[99], A. Farbin[8], A. Farilla[77a], K. Farman[154], T. Farooque[109], J. N. Farr[178], M. S. Farrington[61], S.M. Farrington[137,52], F. Fassi[36e], D. Fassouliotis[9], L. Fayard[66], P. Federic[136], P. Federicova[134], O.L. Fedin[38,p], M. Feickert[176], L. Feligioni[104], D.E. Fellers[18a], C. Feng[143a], Y. Feng[14], Z. Feng[117], M.J. Fenton[165], L. Ferencz[48], B. Fernandez Barbadillo[93], P. Fernandez Martinez[67], M. Bosman[13], M.J.V. Fernoux[104], J. Ferrando[93], A. Ferrari[167], P. Ferrari[117,116], R. Ferrari[73a], D. Ferrere[56], C. Ferretti[108], M. P. Fewell[1], D. Fiacco[75a,75b], F. Fiedler[102], P. Fiedler[135], S. Filimonov[39], M.S. Filip[28b,q], A. Filipčič[95], E.K. Filmer[162a], F. Filthaut[116], L. Fiorini[169], W.C. Fisher[109], T. Fitschen[103], P. M. Fitzhugh[138], I. Fleck[147], P. Fleischmann[108], T. Flick[177], M. Flores[34d,r], L.R. Flores Castillo[64a], L. Flores Sanz De Acedo[37], F.M. Follega[78a,78b], N. Fomin[33], J.H. Foo[161], A. Formica[138], A.C. Forti[103], E. Fortin[37], A.W. Fortman[18a], L. Foster[18a], L. Fountas[9,s], D. Fournier[66], H. Fox[93], P. Francavilla[74a,74b], S. Francescato[61], S. Franchellucci[56], M. Franchini[24b,24a], S. Franchino[63a], D. Francis[37], L. Franco[116], L. Franconi[48], M. Franklin[61], G. Frattari[27], Y.Y. Frid[157], J. Friend[59], N. Fritzsche[37], A. Froch[56], D. Froidevaux[37], J.A. Frost[137], Y. Fu[109], S. Fuenzalida Garrido[140g], M. Fujimoto[151], K. Y. Fung[64a], M. Furukawa[159], J. Fuster[169], A. Gaa[55], A. Gabrielli[24b,24a], A. Gabrielli[161], P. Gadow[37], G. Gagliardi[57b,57a], L.G. Gagnon[18a], S. Gaid[85b], S. Galantzan[157], J. Gallagher[1], E.J. Gallas[129], A.L. Gallen[167], B.J. Gallop[137], K.K. Gan[122], S. Ganguly[159], Y. Gao[52], A. Garabaglu[142], F.M. Garay Walls[140a,140b], C. García[169], A. Garcia Alonso[117], A.G. Garcia Caffaro[178], J.E. García Navarro[169], M. A. Garcia Ruiz[23b], M. Garcia-Sciveres[18a], G.L. Gardner[131], R.W. Gardner[40], N. Garelli[164], R.B. Garg[149], J.M. Gargan[33], C.A. Garner[161], C.M. Garvey[34a], G. Evans[133a,133b], V. K. Gassmann[164], G. Gaudio[73a], V. Gautam[13], P. Gauzzi[75a,75b], J. Gavranovic[95], I.L. Gavrilenko[133a], A. Gavrilyuk[38],

C. Gay[170], G. Gaycken[126], E.N. Gazis[10], A. Gekow[122], C. Gemme[57b], M.H. Genest[60], A. D. Gentry[115], S. George[97], T. Geralis[46], A. A. Gerwin[123], P. Gessinger-Befurt[37], M.E. Geyik[177], M. Ghani[173], K. Ghorbanian[96], A. Ghosal[147], A. Ghosh[165], A. Ghosh[7], B. Giacobbe[24b], S. Giagu[75a,75b], T. Giani[117], A. Giannini[62], S.M. Gibson[97], M. Gignac[139], D.T. Gil[87b], A.K. Gilbert[87a], B.J. Gilbert[42], D. Gillberg[35], G. Gilles[117], D.M. Gingrich[2,t], M.P. Giordani[69a,69c], P.F. Giraud[138], G. Giugliarelli[69a,69c], D. Giugni[71a], F. Giuli[76a,76b], I. Gkialas[9,s], L.K. Gladilin[38], C. Glasman[101], M. Glazewska[20], R. M. Gleason[165], G. Glemža[48], M. Glisic[126], I. Gnesi[44b], Y. Go[30], M. Goblirsch-Kolb[37], B. Gocke[49], D. Godin[110], B. Gokturk[22a], S. Goldfarb[107], T. Golling[56], M.G.D. Gololo[34c], D. Golubkov[38], J.P. Gombas[109], G. Gomes Da Silva[147], A.J. Gomez Delegido[37], L. Gonella[21], A. Gongadze[155c], F. Gonnella[21], J.L. Gonski[149], R.Y. González Andana[52], S. González de la Hoz[169], M. V. Gonzalez Rodrigues[48], S. Gonzalez-Sevilla[56], R. Gonzalez Suarez[167], L. Goossens[37], B. Gorini[37], E. Gorini[70a,70b], A. Gorišek[95], T.C. Gosart[131], A.T. Goshaw[51], M.I. Gostkin[39], S. Goswami[124], C.A. Gottardo[37], S. A. Gotz[111], M. Gouighri[36b], A.G. Goussiou[142], N. Govender[34c], R. P. Grabarczyk[129], I. Grabowska-Bold[87a], K. Graham[35], E. Gramstad[128], S. Grancagnolo[70a,70b], C.M. Grant[1], P.M. Gravila[28f], F.G. Gravili[70a,70b], H.M. Gray[18a], M. Greco[112], M. J. Green[1], C. Grefe[25], A. S. Grefsrud[17], I.M. Gregor[48], R.R. Marcelo Gregorio[96], K.T. Greif[165], P. Grenier[149], S.G. Grewe[112], A.A. Grillo[139], K. Grimm[32], S. Grinstein[13,u], J.-F. Grivaz[66], E. Gross[175], J. Grosse-Knetter[55], L. Guan[108], G. Guerrieri[37], R. Guevara[128], R. Gugel[102], J.A.M. Guhit[108], A. Guida[19], E. Guilloton[173], S. Guindon[37], F. Guo[14,114c], J. Guo[144a], L. Guo[48], L. Guo[114b,v], Y. Guo[108], Y. Guo[42], A. Gupta[49], R. Gupta[132], S. Gupta[27], S. Gurbuz[25], S.S. Gurdasani[48], G. Gustavino[75a,75b], P. Gutierrez[123], L.F. Gutierrez Zagazeta[131], M. Gutsche[50], C. Gutschow[98], C. Gwenlan[129], C.B. Gwilliam[94], E.S. Haaland[128], A. Haas[120], M. Habedank[59], C. Haber[18a], H.K. Hadavand[8], A. Haddad[41], A. Hadef[50], A.I. Hagan[93], J. J. Hahn[147], E.H. Haines[98], M. Haleem[172], J. Haley[124], G.D. Hallewell[104], J.A. Hallford[48], K. Hamano[171], H. Hamdaoui[167], M. Hamer[25], S. E. D. Hammoud[66], E.J. Hampshire[97], J. Han[143a], L. Han[114a], L. Han[62], S. Han[14], K. Hanagaki[84], M. Hance[139], D.A. Hangal[42], H. Hanif[148], M.D. Hank[131], J.B. Hansen[43], P.H. Hansen[43], T. Harenberg[177], S. Harkusha[179], M.L. Harris[105], Y.T. Harris[25], J. Harrison[13], N.M. Harrison[122], P.F. Harrison[173], M. L. E. Hart[98], N.M. Hartman[112], R. Z. Hasan[97,137], Y. Hasegawa[146], F. Haslbeck[129], S. Hassan[17], R. Hauser[109], M. Haviernik[136], C.M. Hawkes[21], R.J. Hawkings[37], Y. Hayashi[159], D. Hayden[109], C. Hayes[108], R.L. Hayes[117], C.P. Hays[129], J.M. Hays[96], H.S. Hayward[94], M. He[14,114c], Y. He[48], Y. He[98], N.B. Heatley[96], V. Hedberg[100], J. Heilman[35], S. Heim[48], T. Heim[18a], J.J. Heinrich[126], L. Heinrich[112], J. Hejbal[134], M. Helbig[50], A. Held[176], S. Hellesund[17], C.M. Helling[170], S. Hellman[47a,47b], A.M. Henriques Correia[37], H. Herde[100], Y. Hernández Jiménez[151], L.M. Herrmann[25], T. Herrmann[50], G. Herten[54], R. Hertenberger[111], L. Hervas[37], M.E. Hesping[102], N.P. Hessey[162a], J. Hessler[112], M. Hidaoui[36b], N. Hidic[136], Y. Nakahama[84], E. Hill[161], T. S. Hillersoy[17], S.J. Hillier[21], J.R. Hinds[109], F. Hinterkeuser[25], M. Hirose[127], S. Hirose[163], D. Hirschbuehl[177], T.G. Hitchings[103], B. Hiti[95], J. Hobbs[151], R. Hobincu[28e], A.M. Hodges[168], M.C. Hodgkinson[145],

JHEP04(2026)020

B.H. Hodkinson[129], A. Hoecker[37], D. D. Hofer[108], J. Hofer[169], J. Hofner[102], M. Holzbock[37], L.B.A.H. Hommels[33], V. Homsak[129], B.P. Honan[103], J. J. Hong[68], T.M. Hong[132], B.H. Hooberman[168], W.H. Hopkins[6], M. C. Hoppesch[168], Y. Horii[113], M. E. Horstmann[112], S. Hou[154], M. R. Housenga[168], J. Howarth[59], J. Hoya[6], M. Hrabovsky[125], T. Hryn'ova[4], P.J. Hsu[65], S.-C. Hsu[142], T. Hsu[66], M. Hu[18a], Q. Hu[62], S. Huang[33], X. Huang[14,114c], Y. Huang[136], Y. Huang[114b], Y. Huang[14], Z. Huang[66], Z. Hubacek[135], F. Huegging[25], T.B. Huffman[129], M. Hufnagel Maranha De Faria[83a], C. A. Hugli[48], M. Huhtinen[37], S.K. Huiberts[128], R. Hulsken[106], C. E. Hultquist[18a], D.L. Humphreys[105], N. Huseynov[12], J. Huston[109], J. Huth[61], L. Huth[48], R. Hyneman[7], G. Iacobucci[56], G. Iakovidis[30], L. Iconomidou-Fayard[66], J. P. Iddon[37], P. Iengo[72a,72b], Y. Iiyama[159], T. Iizawa[159], Y. Ikegami[84], D. Iliadis[158], N. Ilic[161], H. Imam[36a], G. Inacio Goncalves[83d], S. A. Infante Cabanas[140c], T. Ingebretsen Carlson[47a,47b], J. M. Inglis[96], G. Introzzi[73a,73b], M. Iodice[77a], V. Ippolito[75a,75b], R. K. Irwin[94], M. Ishino[159], W. Islam[176], C. Issever[19], S. Istin[22a,w], K. Itabashi[84], H. Ito[174], R. Iuppa[78a,78b], A. Ivina[175], V. Izzo[72a], P. Jacka[135], P. Jackson[1], P. Jain[48], K. Jakobs[54], T. Jakoubek[175], J. Jamieson[59], W. Jang[159], S. Jankovych[136], M. Javurkova[105], P. Jawahar[103], L. Jeanty[126], J. Jejelava[155a,x], P. Jenni[54,y], C.E. Jessiman[35], C. Jia[143a], H. Jia[170], J. Jia[151], X. Jia[112,114c], Z. Jia[114a], C. Jiang[52], Q. Jiang[64b], S. Jiggins[48], M. Jimenez Ortega[169], J. Jimenez Pena[13], S. Jin[114a], A. Jinaru[28b], O. Jinnouchi[141], P. Johansson[145], K.A. Johns[7], J.W. Johnson[139], F. A. Jolly[48], D.M. Jones[152], E. Jones[48], K.S. Jones[8], P. Jones[33], R.W.L. Jones[93], T.J. Jones[94], H.L. Joos[55], R. Joshi[122], J. Jovicevic[16], X. Ju[18a], J.J. Junggeburth[37], T. Junkermann[63a], A. Juste Rozas[13,u], M.K. Juzek[88], S. Kabana[140f], A. Kaczmarska[88], S. A. Kadir[149], M. Kado[112], H. Kagan[122], M. Kagan[149], A. Kahn[131], C. Kahra[102], T. Kaji[159], E. Kajomovitz[156], N. Kakati[175], N. Kakoty[13], I. Kalaitzidou[54], S. Kandel[8], N. Kanellos[10], N.J. Kang[139], D. Kar[34j,†], E. Karentzos[25], K. Karki[8], G. Martinovicova[136], O. Karkout[117], S.N. Karpov[39], Z.M. Karpova[39], V. Kartvelishvili[93,155b], A.N. Karyukhin[38], E. Kasimi[158], J. Katzy[48], S. Kaur[35], K. Kawade[146], M.P. Kawale[123], C. Kawamoto[89], T. Kawamoto[62], E.F. Kay[37], S. Kazakos[109], V.F. Kazanin[38], J.M. Keaveney[34a], R. Keeler[171], G.V. Kehris[61], J.S. Keller[35], J. M. Kelly[171], J.J. Kempster[152], O. Kepka[134], J. Kerr[162b], B.P. Kerridge[137], B.P. Kerševan[95], L. Keszeghova[29a], R. A. Khan[132], A. Khanov[124], A.G. Kharlamov[38], T. Kharlamova[38], E.E. Khoda[142], M. Kholodenko[133a], T.J. Khoo[19], G. Khoriauli[172], Y. Khoulaki[36a], Y.A.R. Khwaira[130], B. Kibirige[34j], D. Kim[6], D.W. Kim[18b], Y.K. Kim[40], N. Kimura[98], M.K. Kingston[55], A. Kirchhoff[55], C. Kirfel[25], F. Kirfel[25], J. Kirk[137], A.E. Kiryunin[112], S. Kita[163], O. Kivernyk[25], M. Klassen[164], C. Klein[35], L. Klein[172], M.H. Klein[45], S.B. Klein[56], U. Klein[94], A. Klimentov[30], T. Klioutchnikova[37], P. Kluit[117], S. Kluth[112], E. Kneringer[79], T.M. Knight[161], A. Knue[49], M. Kobel[50], D. Kobylianskii[175], S.F. Koch[129], M. Kocian[149], D.M. Koeck[126], P. Kodyš[136], K. Köneke[55], T. Koffas[35], O. Kolay[50], I. Koletsou[4], T. Komarek[88], A.X.Y. Kong[1], T. Kono[121], N. Konstantinidis[98], P. Kontaxakis[56], B. Konya[100], R. Kopeliansky[42], S. Koperny[87a], K. Korcyl[88], K. Kordas[158,z], A. Korn[98], S. Korn[55], I. Korolkov[13], N. Korotkova[38], B. Kortman[117], O. Kortner[112], S. Kortner[112], W.H. Kostecka[118], M. Kostov[29a], V.V. Kostyukhin[147], A. Kotsokechagia[37], A. Kotwal[51], A. Koulouris[37], Y. Kulchitsky[39], A. Kourkoumeli-Charalampidi[73a,73b], C. Kourkoumelis[9], E. Kourlitis[112], O. Kovanda[126], R. Kowalewski[171], W. Kozanecki[126], A.S. Kozhin[38], V.A. Kramarenko[38], G. Kramberger[95], P. Kramer[25], M.W. Krasny[130], A. Krasznahorkay[105], A. C. Kraus[118], J.W. Kraus[177], J.A. Kremer[48], N. B. Krengel[147], T. Kresse[50], L. Kretschmann[177], J. Kretzschmar[94], P. Krieger[161], K. Krizka[21], K. Kroeninger[49], H. Kroha[112], J. Kroll[134], J. Kroll[131], K.S. Krowpman[109], U. Kruchonak[39], H. Krüger[25], N.M. Hartmann[111], N. Krumnack[81], M.C. Kruse[51], O. Kuchinskaia[39], S. Kuday[3a], S. Kuehn[37], T. Kuhl[48], V. Kukhtin[39], S. Kuleshov[140d,140b], J. Kull[1], E. V. Kumar[111], M. Kumar[34j], N. Kumari[48], P. Kumari[162b], A. Kupco[134], A. Kupich[38], O. Kuprash[54], H. Kurashige[86], L.L. Kurchaninov[162a], O. Kurdysh[4], A. Kurova[38], R. Kuesters[54], M. Kuze[141], A.K. Kvam[105], J. Kvita[125], N.G. Kyriacou[142], M. Laassiri[30], C. Lacasta[169], F. Lacava[75a,75b], H. Lacker[19], D. Lacour[130], N.N. Lad[98], E. Ladygin[39], A. Lafarge[41], B. Laforge[130], T. Lagouri[178], F.Z. Lahbabi[36a], S. Lai[55,37], W. S. Lai[98], J.E. Lambert[171], S. Lammers[68], W. Lampl[7], C. Lampoudis[158,z], G. Lamprinoudis[172], A.N. Lancaster[118], E. Lançon[30], U. Landgraf[54], M.P.J. Landon[96], V.S. Lang[54], A.J. Lankford[165], F. Lanni[37], K. Lantzsch[25], A. Lanza[73a], M. Lanzac Berrocal[169], J.F. Laporte[138], T. Lari[71a], D. Larsen[17], L. Larson[11], F. Lasagni Manghi[24b], M. Lassnig[37], S.D. Lawlor[145], R. Lazaridou[165], M. Lazzaroni[71a,71b], E. T. T. Le[165], H. D. M. Le[109], E.M. Le Boulicaut[178], L.T. Le Pottier[18a], B. Leban[24b,24a], F. Ledroit-Guillon[60], T.F. Lee[162b], L.L. Leeuw[34c], M. Lefebvre[171], C. Leggett[18a], G. Lehmann Miotto[37], M. Leigh[56], W.A. Leight[105], W. Leinonen[116], A. Leisos[158,aa], C.E. Leitgeb[19], R. Leitner[136], K.J.C. Leney[45], T. Lenz[25], S. Leone[74a], C. Leonidopoulos[52], A. Leopold[150], J. LePage-Bourbonnais[35], R. Les[109], C.G. Lester[33], M. Levchenko[38], J. Levêque[4], L.J. Levinson[175], G. Levrini[24b,24a], M.P. Lewicki[88], C. Lewis[142], D.J. Lewis[4], L. Lewitt[145], A. Li[30], B. Li[143a], C. Li[108], C-Q. Li[112], H. Li[143a], H. Li[103], H. Li[15], H. Li[62], H. Li[143a], J. Li[144a], K. Li[14], L. Li[144a], R. Li[178], S. Li[14,114c], S. Li[144b,144a], T. Li[5], X. Li[106], Y. Li[14], Z. Li[159], Z. Li[14,114c], Z. Li[62], S. Liang[14,114c], Z. Liang[14], M. Liberatore[138], B. Liberti[76a], G. B. Libotte[83d], K. Lie[64c], J. Lieber Marin[83e], H. Lien[68], H. Lin[108], S. F. Lin[151], L. Linden[111], R.E. Lindley[7], J.H. Lindon[37], J. Ling[61], E. Lipeles[131], A. Lipniacka[17], M.A.L. Leite[83c], A. Lister[170], J.D. Little[68], B. Liu[14], B.X. Liu[114b], D. Liu[144b], D. Liu[139], E. H. L. Liu[21], J.K.K. Liu[120], K. Liu[144b], K. Liu[144b,144a], M. Liu[62], M.Y. Liu[62], P. Liu[14], Q. Liu[149], S. Liu[151], X. Liu[62], X. Liu[143a], Y. Liu[114b,114c], Y. Liu[168], Y.L. Liu[143a], Y.W. Liu[62], Z. Liu[66,ab], S.L. Lloyd[96], E.M. Lobodzinska[48], P. Loch[7], E. Lodhi[161], G. Löschcke Centeno[4], K. Lohwasser[145], E. Loiacono[48], J. D. Lomas[21], J.D. Long[42], I. Longarini[165], R. Longo[168], A. Lopez Solis[13], N.A. Lopez-canelas[7], N. Lorenzo Martinez[4], A.M. Lory[111], M. Losada[119a], X. Lou[47a,47b], X. Lou[14,114c], A. Lounis[66], P.A. Love[93], M. Lu[66], S. Lu[131], Y.J. Lu[154], H.J. Lubatti[142], C. Luci[75a,75b], F.L. Lucio Alves[114a], F. Luehring[68], B. S. Lunday[131], O. Lundberg[150], J. Lunde[37], N.A. Luongo[6], M.S. Lutz[37], A.B. Lux[26], D. Lynn[30], R. Lysak[134], V. Lysenko[135], E. Lytken[100], V. Lyubushkin[39], T. Lyubushkina[39], M.M. Lyukova[151], H. Ma[30], K. Ma[62], L.L. Ma[143a],

W. Ma[62], Y. Ma[124], J.C. MacDonald[102], B. Maček[95], P.C. Machado De Abreu Farias[83e], D. Macina[37], R. Madar[41], T. Madula[98], J. Maeda[86], T. Maeno[30], P.T. Mafa[34c,ac], H. Maguire[145], M. Maheshwari[33], V. Maiboroda[66], A. Maio[133a,133b,133d], K. Maj[87a], O. Majersky[48], S. Majewski[126], R. Makhmanazarov[38], N. Makovec[66], V. Maksimovic[16], B. Malaescu[130], J. Malamant[128], Pa. Malecki[88], V.P. Maleev[38], F. Malek[60,ad], M. Mali[95], D. Malito[97], U. Mallik[80,†], A. Maloizel[5], S. Maltezos[10], A. Malvezzi Lopes[83d], S. Malyukov[39], J. Mamuzic[95], G. Mancini[53], M. N. Mancini[27], G. Manco[73a,73b], J.P. Mandalia[96], S.S. Mandarry[152], I. Mandić[95], L. Manhaes de Andrade Filho[83a], I.M. Maniatis[175], J. Manjarres Ramos[91], D.C. Mankad[175], A. Mann[111], T. Manoussos[37], M.N. Mantinan[40], S. Manzoni[37], L. Mao[144a], X. Mapekula[34c], A. Marantis[158], G. Marchiori[5], C. Marcon[71a], E. Maricic[16], M. Marinescu[48], S. Marium[48], M. Marjanovic[123], A. Markhoos[54], M. Markovitch[66], M. K. Maroun[105], M. C. Marr[148], G. T. Marsden[103], E.J. Marshall[93], Z. Marshall[18a], S. Marti-Garcia[169], J. Martin[98], T.A. Martin[137], V.J. Martin[52], B. Martin dit Latour[17], S. Martin-Haugh[137], L. Martinelli[75a,75b], P. Martinez Agullo[169], V.I. Martinez Outschoorn[105], P. Martinez Suarez[37], M. Martinez[13,u], V.S. Martoiu[28b], A.C. Martyniuk[98], A. Marzin[37], D. Mascione[78a,78b], L. Masetti[102], J. Masik[103], A.L. Maslennikov[39], S.L. Mason[42], P. Massarotti[72a,72b], P. Mastrandrea[74a,74b], A. Mastroberardino[44b,44a], T. Masubuchi[127], T.T. Mathew[126], G. Pinheiro Matos[42], J. Matousek[136], D.M. Mattern[49], K. Mauer[48], J. Maurer[28b], T. Maurin[59], A.J. Maury[66], C. Mavungu Tsava[104], D.A. Maximov[38], A. E. May[103], E. Mayer[41], R. Mazini[34j], I. Maznas[118], S.M. Mazza[139], E. Mazzeo[37], R.P. McGovern[131], J.P. Mc Gowan[171], S.P. Mc Kee[108], C.C. McCracken[170], E.F. McDonald[107], A.E. McDougall[117], L. F. Mcelhinney[93], J.A. Mcfayden[152], R.P. Mckenzie[34j], T.C. Mclachlan[48], D.J. Mclaughlin[98], C.A. Mc Lean[6], S.J. McMahon[137], C.M. Mcpartland[94], R.A. McPherson[171,n], S. Mehlhase[111], A. Mehta[94], D. Melini[169], B.R. Mellado Garcia[34j], A.H. Melo[55], F. Meloni[48], A.M. Mendes Jacques Da Costa[103], J.G. Saraiva[133a,133d], L. Meng[93], S. Menke[112], M. Mentink[37], E. Meoni[44b,44a], G. Mercado[118], S. Merianos[158], C. Merlassino[69a,69c], C. Meroni[71a,71b], J. Metcalfe[6], A.S. Mete[6], E. Meuser[102], C. Meyer[68], J-P. Meyer[138], Y. Miao[114a], R.P. Middleton[137], M. Mihovilovic[66], K. Petukhova[37], L. Mijović[52], G. Mikenberg[175], M. Mikestikova[134], M. Mikuž[95], H. Mildner[102], A. Milic[37], D.W. Miller[40], E. H. Miller[149], A. Milov[175], D.A. Milstead[47a,47b], T. Min[114a], A.A. Minaenko[38], I.A. Minashvili[155b], A.I. Mincer[120], B. Mindur[87a], M. Mineev[39], Y. Mino[89], L.M. Mir[13], M. Miralles Lopez[59], M. Mironova[18a], M. Missio[41], A. Mitra[173], V.A. Mitsou[169], Y. Mitsumori[113], O. Miu[161], P.S. Miyagawa[96], T. Mkrtchyan[37], M. Mlinarevic[98], T. Mlinarevic[98], M. Mlynarikova[136], L. Mlynarska[87a], C. Mo[144a], S. Mobius[20], M. H. Mohamed Farook[115], S. Mohapatra[42], S. Mohiuddin[124], G. Mokgatitswane[34j], L. Moleri[175], U. Molinatti[129], L.G. Mollier[20], B. Mondal[134], S. Mondal[135], K. Mönig[48], E. Monnier[104], L. Monsonis Romero[169], J. Montejo Berlingen[13], A. Montella[47a,47b], M. Montella[122], F. Montereali[77a,77b], F. Monticelli[92], S. Monzani[69a,69c], R. Gonçalo[133a], A. Morancho Tarda[43], N. Morange[66], A.L. Moreira De Carvalho[48], M. Moreno Llácer[169], C. Moreno Martinez[56], J.M. Moreno Perez[23b], P. Morettini[57b], S. Morgenstern[37], M. Morii[61], M. Morinaga[159], M. Moritsu[90], F. Morodei[75a,75b], P. Moschovakos[37], B. Moser[54], M. Mosidze[155b],

T. Moskalets[45], P. Moskvitina[116], J. Moss[32], P. Moszkowicz[87a], T. Motta Quirino[83d], A. Moussa[36d], Y. Moyal[175], H. Moyano Gomez[13], E.J.W. Moyse[105], T.G. Mroz[88], S. Muanza[104], M. Mucha[25], J. Mueller[132], G.A. Mullier[167], A.J. Mullin[33], J.J. Mullin[51], A.C. Mullins[45], A.E. Mulski[61], D.P. Mungo[161], D. Munoz Perez[169], F.J. Munoz Sanchez[103], W.J. Murray[173,137], M. Muškinja[95], C. Mwewa[48], A.G. Myagkov[38,p], A.J. Myers[8], G. Myers[108], M. Myska[135], B.P. Nachman[149], K. Nagai[129], K. Nagano[84], R. Nagasaka[159], J.L. Nagle[30,ae], E. Nagy[104], A.M. Nairz[37], K. Nakamura[84], K. Nakkalil[5], A. Nandi[63b], H. Nanjo[127], E.A. Narayanan[45], Y. Narukawa[159], I. Naryshkin[38], L. Nasella[71a,71b], S. Nasri[119b], C. Nass[25], G. Navarro[23a], A. Nayaz[19], P.Y. Nechaeva[38], S. Nechaeva[24b,24a], F. Nechansky[134], L. Nedic[129], T.J. Neep[21], A. Negri[73a,73b], M. Negrini[24b], C. Nellist[117], C. Nelson[106], K. Nelson[108], S. Nemecek[134], M. Nessi[37,af], M.S. Neubauer[168], J. Newell[94], P.R. Newman[21], Y.W.Y. Ng[168], B. Ngair[119a], H.D.N. Nguyen[110], J.D. Nichols[123], R.B. Nickerson[129], J. Nielsen[139], M. Niemeyer[55], J. Niermann[37], N. Nikiforou[37], V. Nikolaenko[38,p], R. Nicolaidou[138], I. Nikolic-Audit[130], P. Nilsson[30], I. Ninca[48], G. Ninio[157], A. Nisati[75a], R. Nisius[112], N. Nitika[175], E.K. Nkadimeng[34b], T. Nobe[159], D. Noll[149], T. Nommensen[153], M.B. Norfolk[145], B.J. Norman[35], L.C. Nosler[18a], M. Noury[36a], J. Novak[95], T. Novak[95], R. Novotny[135], L. Nozka[125], K. Ntekas[165], D. Ntounis[149], N.M.J. Nunes De Moura Junior[83b], A.P. O'Neill[20], J. Ocariz[130], I. Ochoa[133a], J.T. Offermann[40], A. Ogrodnik[88], A. Oh[103], C.C. Ohm[150], H. Oide[84], M.L. Ojeda[37], Y. Okumura[159], I. Oleksiyuk[56], G. Oliveira Correa[13], D. Oliveira Damazio[30], J.L. Oliver[1], R. Omar[68], Ö.O. Öncel[54], Y. Onoda[141], A. Onofre[133a,133e,ag], P.U.E. Onyisi[11], S. Oerdek[48], M.J. Oreglia[40], D. Orestano[77a,77b], R. Orlandini[77a,77b], R.S. Orr[161], L.M. Osojnak[42], Y. Osumi[113], G. Otero y Garzón[31], H. Otono[90], M. Ouchrif[36d], F. Ould-Saada[128], T. Ovsiannikova[142], M. Owen[59], R.E. Owen[137], V.E. Ozcan[22a], F. Ozturk[88], N. Ozturk[8], S. Ozturk[82], H.A. Pacey[129], K. Pachal[162a], A. Pacheco Pages[13], C. Padilla Aranda[13], G. Padovano[75a,75b], S. Pagan Griso[18a], J. Pampel[25], J. Pan[178], D.K. Panchal[11], C.E. Pandini[60], J.G. Panduro Vazquez[137], H.D. Pandya[1], H. Pang[138], P. Pani[48], G. Panizzo[69a,69c], L. Panwar[130], L. Paolozzi[56], S. Parajuli[168], A. Paramonov[6], C. Paraskevopoulos[53], D. Paredes Hernandez[64b], S.R. Paredes Saenz[52], A. Pareti[73a,73b], K.R. Park[42], T.H. Park[112], F. Parodi[57b,57a], J.A. Parsons[42], U. Parzefall[54], B. Pascual Dias[41], L. Pascual Dominguez[101], E. Pasqualucci[75a], S. Passaggio[57b], F. Pastore[97], P. Patel[88], U.M. Patel[51], J.R. Pater[103], T. Pauly[37], F. Pauwels[136], C.I. Pazos[164], M. Pedersen[128], R. Pedro[133a], A.P. Pereira Peixoto[142], S.V. Peleganchuk[38], O. Penc[134], S. Peng[15], G. D. Penn[178], K.E. Penski[111], M. Penzin[38], B.C. Pinheiro Pereira[133a], L. Pereira Sanchez[149], D.V. Perepelitsa[30,ae], G. Perera[105], E. Perez Codina[37], M. Perganti[10], H. Pernegger[37], S. Perrella[75a,75b], K. Peters[48], R.F.Y. Peters[103], B.A. Petersen[37], T.C. Petersen[43], E. Petit[104], V. Petousis[135], A. R. Petri[71a,71b], C. Petridou[158,z], T. Petru[136], M. Pettee[18a], A. Petukhov[82], R. Pezoa[140g], L. Pezzotti[24b,24a], G. Pezzullo[178], L. Pfaffenbichler[37], A. J. Pfleger[79], T.M. Pham[176], T. Pham[107], P.W. Phillips[137], G. Piacquadio[151], E. Pianori[18a], F. Piazza[126], R. Piegaia[31], D. Pietreanu[28b], A.D. Pilkington[103], M. Pinamonti[69a,69c], J.L. Pinfold[2], J. Pinol Bel[13], A. E. Pinto Pinoargote[130], L. Pintucci[69a,69c], K. M. Piper[152],

A. Pirttikoski[56], D.A. Pizzi[35], L. Pizzimento[64b], A. Plebani[33], M.-A. Pleier[30], V. Pleskot[136], E. Plotnikova[39], G. Poddar[96], L. Poggioli[130], S. Polacek[136], G. Polesello[73a], A. Poley[148], A. Polini[24b], C.S. Pollard[173], Z.B. Pollock[122], E. Pompa Pacchi[123], N. I. Pond[98], D. Ponomarenko[68], L. Pontecorvo[37], S. Popa[28a], G.A. Popeneciu[28d], A. Poreba[37], D.M. Portillo Quintero[162a], S. Pospisil[135], M. A. Postill[145], P. Postolache[28c], K. Potamianos[173], P.A. Potepa[87a], I.N. Potrap[39], C.J. Potter[33], R. Poettgen[100], H. Potti[153], J. Poveda[169], M.E. Pozo Astigarraga[37], R. Pozzi[37], A. Prades Ibanez[76a,76b], S.R. Pradhan[145], J. Pretel[171], D. Price[103], M. Primavera[70a], L. Primomo[69a,69c], M.A. Principe Martin[101], R. Privara[125], T. Procter[87b], M.L. Proffitt[142], N. Proklova[131], K. Prokofiev[64c], G. Proto[112], J. Proudfoot[6], M. Przybycien[87a], W.W. Przygoda[87b], A. Psallidas[46], J.E. Puddefoot[145], D. Pudzha[53], E. Egidio Purcino De Souza[83e], H. I. Purnell[1], D. Pyatiizbyantseva[116], J. Qian[108], R. Qian[109], Y. Qin[13], T. Qiu[52], A. Quadt[55], M. Queitsch-Maitland[103], G. Quetant[56], R.P. Quinn[170], G. Rabanal Bolanos[61], D. Rafanoharana[112], F. Raffaeli[76a,76b], F. Ragusa[71a,71b], J.L. Rainbolt[40], S. Rajagopalan[30], E. Ramakoti[39], L. Rambelli[57b,57a], I.A. Ramirez-Berend[35], K. Ran[108,114c], D. S. Rankin[131], N.P. Rapheeha[34j], H. Rasheed[28b], A. Rastogi[18a], S. Rave[102], S. Ravera[57b,57a], B. Ravina[37], I. Ravinovich[175], M. Raymond[37], A.L. Read[128], N.P. Readioff[145], D.M. Rebuzzi[73a,73b], A. S. Reed[59], K. Reeves[27], D. Reikher[37], A. Rej[49], C. Rembser[37], H. Ren[62], M. Renda[28b], F. Renner[48], A.G. Rennie[59], M. Repik[56], A.L. Rescia[57b,57a], S. Resconi[71a], M. Ressegotti[57b], S. Rettie[117], W.F. Rettie[35], M. M. Revering[33], E. Reynolds[18a], O.L. Rezanova[39], P. Reznicek[136], H. Riani[36d], N. Ribaric[51], B. Ricci[69a,69c], E. Ricci[78a,78b], R. Richter[112], S. Richter[47a,47b], E. Richter-Was[87b], M. Ridel[130], S. Ridouani[36d], P. Rieck[120], P. Riedler[37], E.M. Riefel[47a,47b], J. O. Rieger[117], M. Rijssenbeek[151], M. Rimoldi[37], L. Rinaldi[24b,24a], P. Rincke[167,55], G. Ripellino[167], I. Riu[13], J.C. Rivera Vergara[171], F. Rizatdinova[124], E. Rizvi[96], B.R. Roberts[18a], S.S. Roberts[139], D. Robinson[33], A. Robson[59], A. Rocchi[76a,76b], C. Roda[74a,74b], F.A. Rodriguez[118], S. Rodriguez Bosca[37], Y. Rodriguez Garcia[23a], A.M. Rodríguez Vera[118], S. Roe[37], J.T. Roemer[37], O. Røhne[128], R.A. Rojas[37], C.P.A. Roland[130], A. Romaniouk[79], E. Romano[73a,73b], M. Romano[24b], A.C. Romero Hernandez[168], N. Rompotis[94], L. Roos[130], S. Rosati[75a], B.J. Rosser[40], E. Rossi[129], E. Rossi[72a,72b], L.P. Rossi[61], L. Rossini[54], R. Rosten[122], M. Rotaru[28b], R. Roth[37], D. Rousseau[66], D. Rousso[48], S. Roy-Garand[161], A. Rozanov[104], Z. M. A. Rozario[59], Y. Rozen[156], A. Rubio Jimenez[169], V.H. Ruelas Rivera[19], T.A. Ruggeri[1], A. Ruggiero[129], A. Ruiz-Martinez[169], A. Rummler[37], G.B. Rupnik Boero[37], Z. Rurikova[54], N.A. Rusakovich[39], S. Ruscelli[49], H.L. Russell[171], G. Russo[75a,75b], J.P. Rutherfoord[7], S. Rutherford Colmenares[33], M. Rybar[136], P. Rybczynski[87a], A. Ryzhov[45], J.A. Sabater Iglesias[56], H.F-W. Sadrozinski[139], F. Safai Tehrani[75a], S. Saha[1], M. Sahinsoy[82], B. Sahoo[175], A. Saibel[169], B. T. Saifuddin[123], M. Saimpert[138], G.T. Saito[83c], M. Saito[159], T. Saito[159], A. Sala[71a,71b], A. Salnikov[149], J. Salt[169], A. Salvador Salas[157], F. Salvatore[152], A. Salzburger[37], D. Sammel[54], E. Sampson[93], D. Sampsonidis[158,z], D. Sampsonidou[126], M.A.A. Samy[59], J. Sánchez[169], V. Sanchez Sebastian[169], H. Sandaker[128], C.O. Sander[48], J.A. Sandesara[176], M. Sandhoff[177], C. Sandoval[23b], L. Sanfilippo[63a], D.P.C. Sankey[137],

T. Sano[89], A. Sansoni[53], M. Santana Queiroz[18b], L. Santi[37], A.S. Cerqueira[83a], C. Santoni[41], H. Santos[133a,133b], A. Santra[175], E. Sanzani[24b,24a], K.A. Saoucha[85b], J. Sardain[7], A.M. Cooper-Sarkar[129], O. Sasaki[84], K. Sato[163], C. Sauer[37], E. Sauvan[4], P. Savard[161,t], R. Sawada[159], C. Sawyer[137], L. Sawyer[99], A. M. Sayed[27], C. Sbarra[24b], A. Sbrizzi[24b,24a], T. Scanlon[98], J. Schaarschmidt[142], U. Schäfer[102], A.C. Schaffer[66,45], D. Schaile[111], R.D. Schamberger[151], C. Scharf[19], M.M. Schefer[20], D. Scheirich[136], M. Schernau[140f], C. Scheulen[56], C. Schiavi[57b,57a], R. Brener[175], M. Schioppa[44b,44a], B. Schlag[149], S. Schlenker[37], J. Schmeing[177], E. Schmidt[112], M. A. Schmidt[177], K. Schmieden[25], C. Schmitt[102], N. Schmitt[102], S. Schmitt[48], N.A. Schneider[111], L. Schoeffel[138], A. Schoening[63b], P.G. Scholer[35], E. Schopf[147], M. Schott[25], S. Schramm[56], T. Schroer[56], H-C. Schultz-Coulon[63a], M. Schumacher[54], B.A. Schumm[139], Ph. Schune[138], H.R. Schwartz[7], A. Schwartzman[149], T.A. Schwarz[108], Ph. Schwemling[138], R. Schwienhorst[109], F.G. Sciacca[20], A. Sciandra[30], G. Sciolla[27], F. Scuri[74a], L.F. Oleiro Seabra[133a], C.D. Sebastiani[37], K. Sedlaczek[118], S.C. Seidel[115], A. Seiden[139], B.D. Seidlitz[42], C. Seitz[48], J.M. Seixas[83b], G. Sekhniaidze[72a], L. Selem[60], N. Semprini-Cesari[24b,24a], A. Semushin[179], D. Sengupta[56], V. Senthilkumar[169], L. Serin[66], M. Sessa[72a,72b], H. Severini[123], F. Sforza[57b,57a], A. Sfyrla[56], Q. Sha[14], H. Shaddix[118], A.H. Shah[33], R. Shaheen[150], J.D. Shahinian[131], M. Shamim[37], L.Y. Shan[14], M. Shapiro[18a], A. Sharma[37], A.S. Sharma[170], P. Sharma[30], P.B. Shatalov[38], K. Shaw[152], S.M. Shaw[103], G.A. Chelkov[39,p], Q. Shen[14], D.J. Sheppard[148], P. Sherwood[98], L. Shi[98], X. Shi[14], S. Shimizu[84], I.P.J. Shipsey[129,†], S. Shirabe[90], M. Shiyakova[39,ah], M.J. Shochet[40], D.R. Shope[128], B. Shrestha[123], S. Shrestha[122,ai], I. Shreyber[39], M.J. Shroff[171], P. Sicho[134], A.M. Sickles[168], E. Sideras Haddad[34j,166], A. C. Sidley[117], A. Sidoti[24b], F. Siegert[50], Dj. Sijacki[16], F. Sili[62], I. Silva Ferreira[83b], M.V. Silva Oliveira[30], S.B. Silverstein[47a], E. Furtado De Simas Filho[83e], S. Simion[66], R. Simoniello[37], E.L. Simpson[103], H. Simpson[152], L.R. Simpson[6], S. Simsek[82], S. Sindhu[55], P. Sinervo[161], S. N. Singh[27], S. Singh[30], S. Sinha[48], S. Sinha[103], M. Sioli[24b,24a], K. Sioulas[9], I. Siral[37], E. Sitnikova[48], J. Sjölin[47a,47b], A. Skaf[55], E. Skorda[21], P. Skubic[123], M. Slawinska[88], I. Slazyk[17], I. Sliusar[128], V. Smakhtin[175], B.H. Smart[137], S.Yu. Smirnov[140b], Y. Smirnov[82], L.N. Smirnova[38,p], O. Smirnova[100], A.C. Smith[42], D.R. Smith[165], J.L. Smith[103], M. B. Smith[35], R. Smith[149], H. Smitmanns[102], M. Smizanska[93], K. Smolek[135], P. Smolyanskiy[135], A.A. Snesarev[39], H.L. Snoek[117], S. Snyder[30], M.F. Mohd Soberi[52], R. Sobie[171,n], A. Soffer[157], C.A. Solans Sanchez[37], E.Yu. Soldatov[39], U. Soldevila[169], A.A. Solodkov[34j], S. Solomon[27], A. Soloshenko[39], K. Solovieva[54], O.V. Solovyanov[41], P. Sommer[50], A. Sonay[13], A. Sopczak[135], A.L. Sopio[52], F. Sopkova[29b], J. D. Sorenson[115], I.R. Sotarriva Alvarez[141], V. Sothilingam[63a], O. J. Soto Sandoval[140c,140b], B.S. Peralva[83d], S. Sottocornola[68], R. Soualah[85a], Z. Soumaimi[36e], M.J. Da Cunha Sargedas De Sousa[57b,57a], D. South[48], N. Soybelman[175], S. Spagnolo[70a,70b], M. Spalla[112], D. Sperlich[54], B. Spisso[72a,72b], D.P. Spiteri[59], L. Splendori[104], M. Spousta[136], E.J. Staats[35], R. Stamen[63a], E. Stanecka[88], W. Stanek-Maslouska[48], M.V. Stange[50], B. Stanislaus[18a], M.M. Stanitzki[48], E.A. Starchenko[38], G.H. Stark[139], J. Stark[91], P. Staroba[134], P. Starovoitov[85b], R. Staszewski[88], C. Stauch[111], G. Stavropoulos[46], A. Stefl[37], A. Stein[102], P. Steinberg[30],

JHEP04(2026)020

B. Stelzer[148,162a], H.J. Stelzer[132], O. Stelzer[162a], H. Stenzel[58], T.J. Stevenson[152], G.A. Stewart[37], J.R. Stewart[124], G. Stoicea[28b], M. Stolarski[133a], S. Stonjek[112], A. Straessner[50], J. Strandberg[150], S. Strandberg[47a,47b], M. Stratmann[177], M. Strauss[123], T. Strebler[104], P. Strizenec[29b], R. Ströhmer[172], D.M. Strom[126], R. Stroynowski[45], A. Strubig[47a,47b], S.A. Stucci[30], B. Stugu[17], J. Stupak[123], N.A. Styles[48], D. Su[149], S. Su[62], X. Su[62], D. Suchy[29a], A. D. Sudhakar Ponnu[55], K. Sugizaki[131], V.V. Sulin[38], D.M.S. Sultan[129], L. Sultanaliyeva[25], S. Sultansoy[3b], S. Sun[176], W. Sun[14], N. Sur[100], M.R. Sutton[152], M. Svatos[134], P. N. Swallow[33], M. Swiatlowski[162a], A. Swoboda[37], I. Sykora[29a], M. Sykora[136], T. Sykora[136], D. Ta[102], K. Tackmann[48,aj], A. Taffard[165], R. Tafirout[162a], Y. Takubo[84], N. Hod[175], M. Talby[104], A.A. Talyshev[38], K.C. Tam[64b], N.M. Tamir[157], A. Tanaka[159], J. Tanaka[159], R. Tanaka[66], M. Tanasini[151], Z. Tao[170], S. Tapia Araya[140g], S. Tapprogge[102], A. Tarek Abouelfadl Mohamed[37], S. Tarem[156], K. Tariq[14], G. Tarna[37], G.F. Tartarelli[71a], M. J. Tartarin[91], P. Tas[136], M. Tasevsky[134], E. Tassi[44b,44a], A.C. Tate[168], Y. Tayalati[36e,ak], G.N. Taylor[107], W. Taylor[162b], R.J. Taylor Vara[169], A.S. Tegetmeier[91], P. Teixeira-Dias[97], J.J. Teoh[161], K. Terashi[159], J. Terron[101], S. Terzo[13], M. Testa[53], R.J. Teuscher[161,n], A. Thaler[79], O. Theiner[56], T. Theveneaux-Pelzer[104], D.W. Thomas[97], J.P. Thomas[21], E.A. Thompson[18a], P.D. Thompson[21], E. Thomson[131], R. E. Thornberry[45], C. Tian[62], Y. Tian[56], V. Tikhomirov[82], Yu.A. Tikhonov[39], S. Timoshenko[38], D. Timoshyn[136], E.X.L. Ting[1], P. Tipton[178], A. Tishelman-Charny[30], K. Todome[141], S. Todorova-Nova[136], L. Toffolin[69a,69c], M. Togawa[84], J. Tojo[90], S. Tokár[29a], O. Toldaiev[68], G. Tolkachev[104], M. Tomoto[84], L. Tompkins[149,al], E. Torrence[126], H. Torres[91], D. I. Torres Arza[140g], E. Torró Pastor[169], M. Toscani[31], C. Tosciri[40], M. Tost[11], D.R. Tovey[145], T. Trefzger[172], P.M. Tricarico[13], A. Tricoli[30], I.M. Trigger[162a], S. Trincaz-Duvoid[130], D.A. Trischuk[171], A. Tropina[39], D. Truncali[76a,76b], L. Truong[34c], M. Trzebinski[88], A. Trzupek[88], F. Tsai[151], M. Tsai[108], A. Tsiamis[158], P.V. Tsiareshka[39], S. Tsigaridas[162a], A. Tsirigotis[158,aa], V. Tsiskaridze[155a], E.G. Tskhadadze[155a], Y. Tsujikawa[89], I.I. Tsukerman[38], V. Tsulaia[18a], S. Tsuno[84], K. Tsuri[121], D. Tsybychev[151], Y. Tu[64b], A. Tudorache[28b], V. Tudorache[28b], S. B. Tuncay[129], S. Turchikhin[57b,57a], I. Turk Cakir[3a], R. Turra[71a], T. Turtuvshin[39,am], P.M. Tuts[42], S. Tzamarias[158,z], Y. Uematsu[84], F. Ukegawa[163], P.A. Ulloa Poblete[140c,140b], E.N. Umaka[30], G. Unal[37], A. Undrus[30], G. Unel[165], J. Urban[29b], P. Urrejola[140e], G. Usai[8], R. Ushioda[160], M. Usman[110], F. Ustuner[52], Z. Uysal[82], V. Vacek[135], B. Vachon[106], T. Vafeiadis[37], A. Vaitkus[98], C. Valderanis[111], E. Valdes Santurio[47a,47b], M. Valente[37], S. Valentinetti[24b,24a], A. Valero[169], E. Valiente Moreno[169], A. Vallier[91], J.A. Valls Ferrer[169], D. R. Van Arneman[117], E.R. Vandewall[149], A. Van Der Graaf[49], H. Z. Van Der Schyf[34j], P. Van Gemmeren[6], M. Van Rijnbach[37], S. Van Stroud[98], I. Van Vulpen[117], P. Vana[136], M. Vanadia[76a,76b], U. M. Vande Voorde[150], W. Vandelli[37], D. Vannicola[157], L. Vannoli[53], R. Vari[75a], M. Varma[178], E.W. Varnes[7], C. Varni[118], D. Varouchas[66], L. Varriale[169], K.E. Varvell[153], M.E. Vasile[28b], L. Vaslin[84], M. D. Vassilev[149], A. Vasyukov[39], L. M. Vaughan[124], R. Vavricka[136], T. Vazquez Schroeder[13], J. Veatch[32], V. Vecchio[103], M.J. Veen[105], I. Veliscek[30], I. Velkovska[95], L.M. Veloce[161], F. Veloso[133a,133c], A.G. Veltman[52], S. Veneziano[75a], A. Ventura[70a,70b], A. Verbytskyi[112], M. Verducci[74a,74b], C. Vergis[96],

M. Verissimo De Araujo [83b], W. Verkerke [117], J.C. Vermeulen [117], C. Vernieri [149], M. Vessella [165], M.C. Vetterli [148,t], A. Vgenopoulos [102], N. Viaux Maira [140g,an], T. Vickey [145], O.E. Vickey Boeriu [145], G.H.A. Viehhauser [129], L. Vigani [63b], M. Vigl [112], M. Villa [24b,24a], M. Villaplana Perez [169], E.M. Villhauer [40], E. Vilucchi [53], M. Vincent [169], M.G. Vincter [35], A. Visibile [117], A. Visive [117], C. Vittori [37], I. Vivarelli [24b,24a], M.I. Vivas Albornoz [48], E. Voevodina [112], F. Vogel [111], J.C. Voigt [50], P. Vokac [135], Yu. Volkotrub [87b], L. Vomberg [25], E. Von Toerne [25], B. Vormwald [37], K. Vorobev [51], M. Vos [169], K. Voss [147], M. Vozak [37], L. Vozdecky [123], N. Vranjes [16], M. Vranjes Milosavljevic [16], M. Vreeswijk [117], N.K. Vu [144b,144a], R. Vuillermet [37], O. Vujinovic [102], I. Vukotic [40], I. K. Vyas [35], J.F. Wack [33], S. Wada [163], C. Wagner [149], J.M. Wagner [18a], W. Wagner [177], S. Wahdan [177], H. Wahlberg [92], C. H. Waits [123], J. Walder [137], R. Walker [111], K. Walkingshaw Pass [59], W. Walkowiak [147], A. Wall [131], E.J. Wallin [100], T. Wamorkar [18a], K. Wandall-Christensen [169], A. Wang [62], A.Z. Wang [139], C. Wang [102], C. Wang [11], H. Wang [18a], J. Wang [64c], P. Wang [103], P. Wang [98], R. Wang [61], R. Wang [6], S.M. Wang [154], S. Wang [14], T. Wang [116], T. Wang [62], W.T. Wang [129], W. Wang [14], X. Wang [168], X. Wang [144a], X. Wang [48], Y. Wang [151], Y. Wang [62], Z. Wang [108], Z. Wang [144b], Z. Wang [108], C. Wanotayaroj [84], A. Warburton [106], A.L. Warnerbring [147], S. Waterhouse [97], A.T. Watson [21], H. Watson [52], M.F. Watson [21], E. Watton [37], G. Watts [142], B.M. Waugh [98], J. M. Webb [54], C. Weber [30], H. A. Weber [19], M.S. Weber [20], S.M. Weber [63a], C. Wei [62], Y. Wei [54], A.R. Weidberg [129], E.J. Weik [120], J. Weingarten [49], C. Weiser [54], C.J. Wells [48], T. Wenaus [30], T. Wengler [37], N.S. Wenke [112], N. Wermes [25], M. Wessels [63a], A.M. Wharton [93], A.S. White [61], A. White [8], M.J. White [1], D. Whiteson [165], L. Wickremasinghe [127], W. Wiedenmann [176], M. Wielers [137], R. Wierda [150], C. Wiglesworth [43], H.G. Wilkens [37], J. J. H. Wilkinson [33], D.M. Williams [42], H.H. Williams [131], S. Williams [33], S. Willocq [105], B.J. Wilson [103], D.J. Wilson [103], P.J. Windischhofer [40], F.I. Winkel [31], F. Winklmeier [126], B.T. Winter [54], M. Wittgen [149], M. Wobisch [99], T. Wojtkowski [60], Z. Wolffs [117], J. Wollrath [37], M.W. Wolter [88], H. Wolters [133a,133c], M.C. Wong [139], E.L. Woodward [42], S.D. Worm [48], B.K. Wosiek [88], K.W. Woźniak [88], S. Wozniewski [55], K. Wraight [59], C. Wu [161], C. Wu [21], J. Wu [159], M. Wu [114b], M. Wu [116], S.L. Wu [176], S. Wu [14,ao], X. Wu [62], Y.Q. Wu [161], Y. Wu [62], Z. Wu [4], Z. Wu [114a], J. Wuerzinger [112], T.R. Wyatt [103], B.M. Wynne [52], S. Xella [43], L. Xia [114a], M. Xie [62], A. Xiong [126], D. Xu [14], H. Xu [62], L. Xu [62], R. Xu [131], T. Xu [108], Y. Xu [142], Z. Xu [52], R. Xue [132], B. Yabsley [153], S. Yacoob [34a], Y. Yamaguchi [84], E. Yamashita [159], H. Yamauchi [163], T. Yamazaki [18a], Y. Yamazaki [86], S. Yan [59], Z. Yan [105], H.J. Yang [144a,144b], H.T. Yang [62], S. Yang [62], T. Yang [64c], X. Yang [37], X. Yang [14], Y. Yang [159], Y. Yang [62], W-M. Yao [18a], C. L. Yardley [152], J. Ye [14], S. Ye [30], X. Ye [62], Y. Yeh [98], I. Yeletskikh [39], B. Yeo [18b], M.R. Yexley [98], T. P. Yildirim [129], H. Duran Yildiz [3a], K. Yorita [174], C.J.S. Young [37], C. Young [149], N.D. Young [126], Y. Yu [62], J. Yuan [14,114c,ao], M. Yuan [108], R. Yuan [144b], L. Yue [98], M. Zaazoua [62], B. Zabinski [88], I. Zahir [36a], A. Zaio [57b,57a], Z.K. Zak [88], T. Zakareishvili [169], S. Zambito [56], J.A. Zamora Saa [140d], J. Zang [159], R. Zanzottera [71a,71b], O. Zaplatilek [135], C. Zeitnitz [177], H. Zeng [14], D.T. Zenger Jr [27], O. Zenin [38], T. Ženiš [29a], S. Zenz [96], D. Zerwas [66], M. Zhai [14,114c], D.F. Zhang [145], G. Zhang [14,ao], J. Zhang [143a], J. Zhang [6], L. Zhang [62], L. Zhang [114a], P. Zhang [14,114c], R. Zhang [114a], S. Zhang [91], T. Zhang [159], Y. Zhang [142],

Y. Zhang[98], Y. Zhang[62], Y. Zhang[114a], Z. Zhang[18a], Z. Zhang[143a], Z. Zhang[66], H. Zhao[142], T. Zhao[143a], Y. Zhao[35], Z. Zhao[62], Z. Zhao[62], A. Zhemchugov[39], J. Zheng[114a], K. Zheng[168], X. Zheng[62], Z. Zheng[149], D. Zhong[168], B. Zhou[108], H. Zhou[7], N. Zhou[144a], Y. Zhou[15], Y. Zhou[114a], Y. Zhou[7], J. Zhu[108], X. Zhu[144b], Y. Zhu[144a], Y. Zhu[62], X. Zhuang[14], K. Zhukov[68], N.I. Zimine[39], J. Zinsser[63b], M. Ziolkowski[147], L. Živković[16], A. Zoccoli[24b,24a], K. Zoch[61], A. Zografos[37], T.G. Zorbas[145], O. Zormpa[46], L. Zwalinski[37]

[1] *Department of Physics, University of Adelaide, Adelaide, Australia*
[2] *Department of Physics, University of Alberta, Edmonton AB, Canada*
[3a] *Department of Physics, Ankara University, Ankara, Türkiye*
[3b] *Division of Physics, TOBB University of Economics and Technology, Ankara, Türkiye*
[4] *LAPP, Université Savoie Mont Blanc, CNRS/IN2P3, Annecy, France*
[5] *APC, Université Paris Cité, CNRS/IN2P3, Paris, France*
[6] *High Energy Physics Division, Argonne National Laboratory, Argonne IL, U.S.A.*
[7] *Department of Physics, University of Arizona, Tucson AZ, U.S.A.*
[8] *Department of Physics, University of Texas at Arlington, Arlington TX, U.S.A.*
[9] *Physics Department, National and Kapodistrian University of Athens, Athens, Greece*
[10] *Physics Department, National Technical University of Athens, Zografou, Greece*
[11] *Department of Physics, University of Texas at Austin, Austin TX, U.S.A.*
[12] *Institute of Physics, Azerbaijan Academy of Sciences, Baku, Azerbaijan*
[13] *Institut de Física d'Altes Energies (IFAE), Barcelona Institute of Science and Technology, Barcelona, Spain*
[14] *Institute of High Energy Physics, Chinese Academy of Sciences, Beijing, China*
[15] *Physics Department, Tsinghua University, Beijing, China*
[16] *Institute of Physics, University of Belgrade, Belgrade, Serbia*
[17] *Department for Physics and Technology, University of Bergen, Bergen, Norway*
[18a] *Physics Division, Lawrence Berkeley National Laboratory, Berkeley CA, U.S.A.*
[18b] *University of California, Berkeley CA, U.S.A.*
[19] *Institut für Physik, Humboldt Universität zu Berlin, Berlin, Germany*
[20] *Albert Einstein Center for Fundamental Physics and Laboratory for High Energy Physics, University of Bern, Bern, Switzerland*
[21] *School of Physics and Astronomy, University of Birmingham, Birmingham, U.K.*
[22a] *Department of Physics, Bogazici University, Istanbul, Türkiye*
[22b] *Department of Physics Engineering, Gaziantep University, Gaziantep, Türkiye*
[22c] *Department of Physics, Istanbul University, Istanbul, Türkiye*
[23a] *Facultad de Ciencias y Centro de Investigaciónes, Universidad Antonio Nariño, Bogotá, Colombia*
[23b] *Departamento de Física, Universidad Nacional de Colombia, Bogotá, Colombia*
[24a] *Dipartimento di Fisica e Astronomia A. Righi, Università di Bologna, Bologna, Italy*
[24b] *INFN Sezione di Bologna, Italy*
[25] *Physikalisches Institut, Universität Bonn, Bonn, Germany*
[26] *Department of Physics, Boston University, Boston MA, U.S.A.*
[27] *Department of Physics, Brandeis University, Waltham MA, U.S.A.*
[28a] *Transilvania University of Brasov, Brasov, Romania*
[28b] *Horia Hulubei National Institute of Physics and Nuclear Engineering, Bucharest, Romania*
[28c] *Department of Physics, Alexandru Ioan Cuza University of Iasi, Iasi, Romania*
[28d] *National Institute for Research and Development of Isotopic and Molecular Technologies, Physics Department, Cluj-Napoca, Romania*
[28e] *National University of Science and Technology Politechnica, Bucharest, Romania*
[28f] *West University in Timisoara, Timisoara, Romania*
[28g] *Faculty of Physics, University of Bucharest, Bucharest, Romania*
[29a] *Faculty of Mathematics, Physics and Informatics, Comenius University, Bratislava, Slovak Republic*

[29b] *Department of Subnuclear Physics, Institute of Experimental Physics of the Slovak Academy of Sciences, Kosice, Slovak Republic*
[30] *Physics Department, Brookhaven National Laboratory, Upton NY, U.S.A.*
[31] *Universidad de Buenos Aires, Facultad de Ciencias Exactas y Naturales, Departamento de Física, y CONICET, Instituto de Física de Buenos Aires (IFIBA), Buenos Aires, Argentina*
[32] *California State University, CA, U.S.A.*
[33] *Cavendish Laboratory, University of Cambridge, Cambridge, U.K.*
[34a] *Department of Physics, University of Cape Town, Cape Town, South Africa*
[34b] *iThemba Labs, Western Cape, South Africa*
[34c] *Department of Mechanical Engineering Science, University of Johannesburg, Johannesburg, South Africa*
[34d] *National Institute of Physics, University of the Philippines Diliman (Philippines), Philippines*
[34e] *Department of Physics, Stellenbosch University, Matieland, South Africa*
[34f] *University of KwaZulu-Natal, School of Agriculture and Science, Mathematics, Westville, South Africa*
[34g] *University of South Africa, Department of Physics, Pretoria, South Africa*
[34h] *University of Pretoria, Department of Mechanical and Aeronautical Engineering, Pretoria, South Africa*
[34i] *University of Zululand, KwaDlangezwa, South Africa*
[34j] *School of Physics, University of the Witwatersrand, Johannesburg, South Africa*
[35] *Department of Physics, Carleton University, Ottawa ON, Canada*
[36a] *Faculté des Sciences Ain Chock, Université Hassan II de Casablanca, Morocco*
[36b] *Faculté des Sciences, Université Ibn-Tofail, Kénitra, Morocco*
[36c] *Faculté des Sciences Semlalia, Université Cadi Ayyad, LPHEA-Marrakech, Morocco*
[36d] *LPMR, Faculté des Sciences, Université Mohamed Premier, Oujda, Morocco*
[36e] *Faculté des sciences, Université Mohammed V, Rabat, Morocco*
[36f] *Institute of Applied Physics, Mohammed VI Polytechnic University, Ben Guerir, Morocco*
[37] *CERN, Geneva, Switzerland*
[38] *Affiliated with an institute formerly covered by a cooperation agreement with CERN*
[39] *Affiliated with an international laboratory covered by a cooperation agreement with CERN*
[40] *Enrico Fermi Institute, University of Chicago, Chicago IL, U.S.A.*
[41] *LPC, Université Clermont Auvergne, CNRS/IN2P3, Clermont-Ferrand, France*
[42] *Nevis Laboratory, Columbia University, Irvington NY, U.S.A.*
[43] *Niels Bohr Institute, University of Copenhagen, Copenhagen, Denmark*
[44a] *Dipartimento di Fisica, Università della Calabria, Rende, Italy*
[44b] *INFN Gruppo Collegato di Cosenza, Laboratori Nazionali di Frascati, Italy*
[45] *Physics Department, Southern Methodist University, Dallas TX, U.S.A.*
[46] *National Centre for Scientific Research "Demokritos", Agia Paraskevi, Greece*
[47a] *Department of Physics, Stockholm University, Sweden*
[47b] *Oskar Klein Centre, Stockholm, Sweden*
[48] *Deutsches Elektronen-Synchrotron DESY, Hamburg and Zeuthen, Germany*
[49] *Fakultät Physik, Technische Universität Dortmund, Dortmund, Germany*
[50] *Institut für Kern- und Teilchenphysik, Technische Universität Dresden, Dresden, Germany*
[51] *Department of Physics, Duke University, Durham NC, U.S.A.*
[52] *SUPA — School of Physics and Astronomy, University of Edinburgh, Edinburgh, U.K.*
[53] *INFN e Laboratori Nazionali di Frascati, Frascati, Italy*
[54] *Physikalisches Institut, Albert-Ludwigs-Universität Freiburg, Freiburg, Germany*
[55] *II. Physikalisches Institut, Georg-August-Universität Göttingen, Göttingen, Germany*
[56] *Département de Physique Nucléaire et Corpusculaire, Université de Genève, Genève, Switzerland*
[57a] *Dipartimento di Fisica, Università di Genova, Genova, Italy*
[57b] *INFN Sezione di Genova, Italy*
[58] *II. Physikalisches Institut, Justus-Liebig-Universität Giessen, Giessen, Germany*
[59] *SUPA — School of Physics and Astronomy, University of Glasgow, Glasgow, U.K.*
[60] *LPSC, Université Grenoble Alpes, CNRS/IN2P3, Grenoble INP, Grenoble, France*
[61] *Laboratory for Particle Physics and Cosmology, Harvard University, Cambridge MA, U.S.A.*

[62] *Department of Modern Physics and State Key Laboratory of Particle Detection and Electronics, University of Science and Technology of China, Hefei, China*
[63a] *Kirchhoff-Institut für Physik, Ruprecht-Karls-Universität Heidelberg, Heidelberg, Germany*
[63b] *Physikalisches Institut, Ruprecht-Karls-Universität Heidelberg, Heidelberg, Germany*
[64a] *Department of Physics, Chinese University of Hong Kong, Shatin, N.T., Hong Kong, China*
[64b] *Department of Physics, University of Hong Kong, Hong Kong, China*
[64c] *Department of Physics and Institute for Advanced Study, Hong Kong University of Science and Technology, Clear Water Bay, Kowloon, Hong Kong, China*
[65] *Department of Physics, National Tsing Hua University, Hsinchu, Taiwan*
[66] *IJCLab, Université Paris-Saclay, CNRS/IN2P3, 91405, Orsay, France*
[67] *Centro Nacional de Microelectrónica (IMB-CNM-CSIC), Barcelona, Spain*
[68] *Department of Physics, Indiana University, Bloomington IN, U.S.A.*
[69a] *INFN Gruppo Collegato di Udine, Sezione di Trieste, Udine, Italy*
[69b] *ICTP, Trieste, Italy*
[69c] *Dipartimento Politecnico di Ingegneria e Architettura, Università di Udine, Udine, Italy*
[70a] *INFN Sezione di Lecce, Italy*
[70b] *Dipartimento di Matematica e Fisica, Università del Salento, Lecce, Italy*
[71a] *INFN Sezione di Milano, Italy*
[71b] *Dipartimento di Fisica, Università di Milano, Milano, Italy*
[72a] *INFN Sezione di Napoli, Italy*
[72b] *Dipartimento di Fisica, Università di Napoli, Napoli, Italy*
[73a] *INFN Sezione di Pavia, Italy*
[73b] *Dipartimento di Fisica, Università di Pavia, Pavia, Italy*
[74a] *INFN Sezione di Pisa, Italy*
[74b] *Dipartimento di Fisica E. Fermi, Università di Pisa, Pisa, Italy*
[75a] *INFN Sezione di Roma, Italy*
[75b] *Dipartimento di Fisica, Sapienza Università di Roma, Roma, Italy*
[76a] *INFN Sezione di Roma Tor Vergata, Italy*
[76b] *Dipartimento di Fisica, Università di Roma Tor Vergata, Roma, Italy*
[77a] *INFN Sezione di Roma Tre, Italy*
[77b] *Dipartimento di Matematica e Fisica, Università Roma Tre, Roma, Italy*
[78a] *INFN-TIFPA, Italy*
[78b] *Università degli Studi di Trento, Trento, Italy*
[79] *Universität Innsbruck, Department of Astro and Particle Physics, Innsbruck, Austria*
[80] *University of Iowa, Iowa City IA, U.S.A.*
[81] *Department of Physics and Astronomy, Iowa State University, Ames IA, U.S.A.*
[82] *Istinye University, Sariyer, Istanbul, Türkiye*
[83a] *Departamento de Engenharia Elétrica, Universidade Federal de Juiz de Fora (UFJF), Juiz de Fora, Brazil*
[83b] *Universidade Federal do Rio De Janeiro COPPE/EE/IF, Rio de Janeiro, Brazil*
[83c] *Instituto de Física, Universidade de São Paulo, São Paulo, Brazil*
[83d] *Rio de Janeiro State University, Rio de Janeiro, Brazil*
[83e] *Federal University of Bahia, Bahia, Brazil*
[84] *KEK, High Energy Accelerator Research Organization, Tsukuba, Japan*
[85a] *Khalifa University of Science and Technology, Abu Dhabi, United Arab Emirates*
[85b] *University of Sharjah, Sharjah, United Arab Emirates*
[86] *Graduate School of Science, Kobe University, Kobe, Japan*
[87a] *AGH University of Krakow, Faculty of Physics and Applied Computer Science, Krakow, Poland*
[87b] *Marian Smoluchowski Institute of Physics, Jagiellonian University, Krakow, Poland*
[88] *Institute of Nuclear Physics Polish Academy of Sciences, Krakow, Poland*
[89] *Faculty of Science, Kyoto University, Kyoto, Japan*
[90] *Research Center for Advanced Particle Physics and Department of Physics, Kyushu University, Fukuoka, Japan*
[91] *L2IT, Université de Toulouse, CNRS/IN2P3, UPS, Toulouse, France*

[92] *Instituto de Física La Plata, Universidad Nacional de La Plata and CONICET, La Plata, Argentina*
[93] *Physics Department, Lancaster University, Lancaster, U.K.*
[94] *Oliver Lodge Laboratory, University of Liverpool, Liverpool, U.K.*
[95] *Department of Experimental Particle Physics, Jožef Stefan Institute and Department of Physics, University of Ljubljana, Ljubljana, Slovenia*
[96] *Department of Physics and Astronomy, Queen Mary University of London, London, U.K.*
[97] *Department of Physics, Royal Holloway University of London, Egham, U.K.*
[98] *Department of Physics and Astronomy, University College London, London, U.K.*
[99] *Louisiana Tech University, Ruston LA, U.S.A.*
[100] *Fysiska institutionen, Lunds universitet, Lund, Sweden*
[101] *Departamento de Física Teorica C-15 and CIAFF, Universidad Autónoma de Madrid, Madrid, Spain*
[102] *Institut für Physik, Universität Mainz, Mainz, Germany*
[103] *School of Physics and Astronomy, University of Manchester, Manchester, U.K.*
[104] *CPPM, Aix-Marseille Université, CNRS/IN2P3, Marseille, France*
[105] *Department of Physics, University of Massachusetts, Amherst MA, U.S.A.*
[106] *Department of Physics, McGill University, Montreal QC, Canada*
[107] *School of Physics, University of Melbourne, Victoria, Australia*
[108] *Department of Physics, University of Michigan, Ann Arbor MI, U.S.A.*
[109] *Department of Physics and Astronomy, Michigan State University, East Lansing MI, U.S.A.*
[110] *Group of Particle Physics, University of Montreal, Montreal QC, Canada*
[111] *Fakultät für Physik, Ludwig-Maximilians-Universität München, München, Germany*
[112] *Max-Planck-Institut für Physik (Werner-Heisenberg-Institut), München, Germany*
[113] *Graduate School of Science and Kobayashi-Maskawa Institute, Nagoya University, Nagoya, Japan*
[114a] *Department of Physics, Nanjing University, Nanjing, China*
[114b] *School of Science, Shenzhen Campus of Sun Yat-sen University, China*
[114c] *University of Chinese Academy of Science (UCAS), Beijing, China*
[115] *Department of Physics and Astronomy, University of New Mexico, Albuquerque NM, U.S.A.*
[116] *Institute for Mathematics, Astrophysics and Particle Physics, Radboud University/Nikhef, Nijmegen, Netherlands*
[117] *Nikhef National Institute for Subatomic Physics and University of Amsterdam, Amsterdam, Netherlands*
[118] *Department of Physics, Northern Illinois University, DeKalb IL, U.S.A.*
[119a] *New York University Abu Dhabi, Abu Dhabi, United Arab Emirates*
[119b] *United Arab Emirates University, Al Ain, United Arab Emirates*
[120] *Department of Physics, New York University, New York NY, U.S.A.*
[121] *Ochanomizu University, Otsuka, Bunkyo-ku, Tokyo, Japan*
[122] *Ohio State University, Columbus OH, U.S.A.*
[123] *Homer L. Dodge Department of Physics and Astronomy, University of Oklahoma, Norman OK, U.S.A.*
[124] *Department of Physics, Oklahoma State University, Stillwater OK, U.S.A.*
[125] *Palacký University, Joint Laboratory of Optics, Olomouc, Czech Republic*
[126] *Institute for Fundamental Science, University of Oregon, Eugene, OR, U.S.A.*
[127] *Graduate School of Science, University of Osaka, Osaka, Japan*
[128] *Department of Physics, University of Oslo, Oslo, Norway*
[129] *Department of Physics, Oxford University, Oxford, U.K.*
[130] *LPNHE, Sorbonne Université, Université Paris Cité, CNRS/IN2P3, Paris, France*
[131] *Department of Physics, University of Pennsylvania, Philadelphia PA, U.S.A.*
[132] *Department of Physics and Astronomy, University of Pittsburgh, Pittsburgh PA, U.S.A.*
[133a] *Laboratório de Instrumentação e Física Experimental de Partículas — LIP, Lisboa, Portugal*
[133b] *Departamento de Física, Faculdade de Ciências, Universidade de Lisboa, Lisboa, Portugal*
[133c] *Departamento de Física, Universidade de Coimbra, Coimbra, Portugal*
[133d] *Centro de Física Nuclear da Universidade de Lisboa, Lisboa, Portugal*
[133e] *Departamento de Física, Escola de Ciências, Universidade do Minho, Braga, Portugal*
[133f] *Departamento de Física Teórica y del Cosmos, Universidad de Granada, Granada (Spain), Spain*
[133g] *Departamento de Física, Instituto Superior Técnico, Universidade de Lisboa, Lisboa, Portugal*

JHEP04(2026)020

[134] *Institute of Physics of the Czech Academy of Sciences, Prague, Czech Republic*
[135] *Czech Technical University in Prague, Prague, Czech Republic*
[136] *Charles University, Faculty of Mathematics and Physics, Prague, Czech Republic*
[137] *Particle Physics Department, Rutherford Appleton Laboratory, Didcot, U.K.*
[138] *IRFU, CEA, Université Paris-Saclay, Gif-sur-Yvette, France*
[139] *Santa Cruz Institute for Particle Physics, University of California Santa Cruz, Santa Cruz CA, U.S.A.*
[140a] *Departamento de Física, Pontificia Universidad Católica de Chile, Santiago, Chile*
[140b] *Millennium Institute for Subatomic physics at high energy frontier (SAPHIR), Santiago, Chile*
[140c] *Instituto de Investigación Multidisciplinario en Ciencia y Tecnología, y Departamento de Física, Universidad de La Serena, Chile*
[140d] *Universidad Andres Bello, Department of Physics, Santiago, Chile*
[140e] *Universidad San Sebastian, Recoleta, Chile*
[140f] *Instituto de Alta Investigación, Universidad de Tarapacá, Arica, Chile*
[140g] *Departamento de Física, Universidad Técnica Federico Santa María, Valparaíso, Chile*
[141] *Department of Physics, Institute of Science, Tokyo, Japan*
[142] *Department of Physics, University of Washington, Seattle WA, U.S.A.*
[143a] *Institute of Frontier and Interdisciplinary Science and Key Laboratory of Particle Physics and Particle Irradiation (MOE), Shandong University, Qingdao, China*
[143b] *School of Physics, Zhengzhou University, China*
[144a] *State Key Laboratory of Dark Matter Physics, School of Physics and Astronomy, Shanghai Jiao Tong University, Key Laboratory for Particle Astrophysics and Cosmology (MOE), SKLPPC, Shanghai, China*
[144b] *State Key Laboratory of Dark Matter Physics, Tsung-Dao Lee Institute, Shanghai Jiao Tong University, Shanghai, China*
[145] *Department of Physics and Astronomy, University of Sheffield, Sheffield, U.K.*
[146] *Department of Physics, Shinshu University, Nagano, Japan*
[147] *Department Physik, Universität Siegen, Siegen, Germany*
[148] *Department of Physics, Simon Fraser University, Burnaby BC, Canada*
[149] *SLAC National Accelerator Laboratory, Stanford CA, U.S.A.*
[150] *Department of Physics, Royal Institute of Technology, Stockholm, Sweden*
[151] *Departments of Physics and Astronomy, Stony Brook University, Stony Brook NY, U.S.A.*
[152] *Department of Physics and Astronomy, University of Sussex, Brighton, U.K.*
[153] *School of Physics, University of Sydney, Sydney, Australia*
[154] *Institute of Physics, Academia Sinica, Taipei, Taiwan*
[155a] *E. Andronikashvili Institute of Physics, Iv. Javakhishvili Tbilisi State University, Tbilisi, Georgia*
[155b] *High Energy Physics Institute, Tbilisi State University, Tbilisi, Georgia*
[155c] *University of Georgia, Tbilisi, Georgia*
[156] *Department of Physics, Technion, Israel Institute of Technology, Haifa, Israel*
[157] *Raymond and Beverly Sackler School of Physics and Astronomy, Tel Aviv University, Tel Aviv, Israel*
[158] *Department of Physics, Aristotle University of Thessaloniki, Thessaloniki, Greece*
[159] *International Center for Elementary Particle Physics and Department of Physics, University of Tokyo, Tokyo, Japan*
[160] *Graduate School of Science and Technology, Tokyo Metropolitan University, Tokyo, Japan*
[161] *Department of Physics, University of Toronto, Toronto ON, Canada*
[162a] *TRIUMF, Vancouver BC, Canada*
[162b] *Department of Physics and Astronomy, York University, Toronto ON, Canada*
[163] *Division of Physics and Tomonaga Center for the History of the Universe, Faculty of Pure and Applied Sciences, University of Tsukuba, Tsukuba, Japan*
[164] *Department of Physics and Astronomy, Tufts University, Medford MA, U.S.A.*
[165] *Department of Physics and Astronomy, University of California Irvine, Irvine CA, U.S.A.*
[166] *University of West Attica, Athens, Greece*
[167] *Department of Physics and Astronomy, University of Uppsala, Uppsala, Sweden*
[168] *Department of Physics, University of Illinois, Urbana IL, U.S.A.*
[169] *Instituto de Física Corpuscular (IFIC), Centro Mixto Universidad de Valencia — CSIC, Valencia, Spain*

JHEP04(2026)020

[170] Department of Physics, University of British Columbia, Vancouver BC, Canada
[171] Department of Physics and Astronomy, University of Victoria, Victoria BC, Canada
[172] Fakultät für Physik und Astronomie, Julius-Maximilians-Universität Würzburg, Würzburg, Germany
[173] Department of Physics, University of Warwick, Coventry, U.K.
[174] Waseda University, Tokyo, Japan
[175] Department of Particle Physics and Astrophysics, Weizmann Institute of Science, Rehovot, Israel
[176] Department of Physics, University of Wisconsin, Madison WI, U.S.A.
[177] Fakultät für Mathematik und Naturwissenschaften, Fachgruppe Physik, Bergische Universität Wuppertal, Wuppertal, Germany
[178] Department of Physics, Yale University, New Haven CT, U.S.A.
[179] Yerevan Physics Institute, Yerevan, Armenia

[a] Also at Department of Physics, King's College London, London, U.K.
[b] Also at Institute of Physics, Azerbaijan Academy of Sciences, Baku, Azerbaijan
[c] Also at Imam Mohammad Ibn Saud Islamic University, Saudi Arabia
[d] Also at Department of Physics, University of Thessaly, Greece
[e] Also at An-Najah National University, Nablus, Palestine
[f] Also at Department of Physics, University of Fribourg, Fribourg, Switzerland
[g] Also at Department of Physics, Westmont College, Santa Barbara, U.S.A.
[h] Also at Departament de Fisica de la Universitat Autonoma de Barcelona, Barcelona, Spain
[i] Also at Borough of Manhattan Community College, City University of New York, New York NY, U.S.A.
[j] Also at University of Siena, Italy
[k] Also at The Collaborative Innovation Center of Quantum Matter (CICQM), Beijing, China
[l] Also at Faculty of Physics, Sofia University, 'St. Kliment Ohridski', Sofia, Bulgaria
[m] Also at Università di Napoli Parthenope, Napoli, Italy
[n] Also at Institute of Particle Physics (IPP), Canada
[o] Also at Department of Physics, Bolu Abant Izzet Baysal University, Bolu, Türkiye
[p] Also at Affiliated with an institute formerly covered by a cooperation agreement with CERN
[q] Also at Faculty of Physics, University of Bucharest, Romania
[r] Also at National Institute of Physics, University of the Philippines Diliman (Philippines), Philippines
[s] Also at Department of Financial and Management Engineering, University of the Aegean, Chios, Greece
[t] Also at TRIUMF, Vancouver BC, Canada
[u] Also at Institucio Catalana de Recerca i Estudis Avancats, ICREA, Barcelona, Spain
[v] Also at Henan University, China
[w] Also at Yeditepe University, Physics Department, Istanbul, Türkiye
[x] Also at Institute of Theoretical Physics, Ilia State University, Tbilisi, Georgia
[y] Also at CERN, Geneva, Switzerland
[z] Also at Center for Interdisciplinary Research and Innovation (CIRI-AUTH), Thessaloniki, Greece
[aa] Also at Hellenic Open University, Patras, Greece
[ab] Also at Department of Modern Physics and State Key Laboratory of Particle Detection and Electronics, University of Science and Technology of China, Hefei, China
[ac] Also at Department of Mathematical Sciences, University of South Africa, Johannesburg, South Africa
[ad] Also at Department of Physics, Stellenbosch University, South Africa
[ae] Also at University of Colorado Boulder, Department of Physics, Colorado, U.S.A.
[af] Also at Département de Physique Nucléaire et Corpusculaire, Université de Genève, Genève, Switzerland
[ag] Also at Centre of Physics of the Universities of Minho and Porto (CF-UM-UP), Portugal
[ah] Also at Institute for Nuclear Research and Nuclear Energy (INRNE) of the Bulgarian Academy of Sciences, Sofia, Bulgaria
[ai] Also at Washington College, Chestertown, MD, U.S.A.
[aj] Also at Institut für Experimentalphysik, Universität Hamburg, Hamburg, Germany
[ak] Also at Institute of Applied Physics, Mohammed VI Polytechnic University, Ben Guerir, Morocco
[al] Also at Department of Physics, Stanford University, Stanford CA, U.S.A.
[am] Also at Institute of Physics and Technology, Mongolian Academy of Sciences, Ulaanbaatar, Mongolia

JHEP04(2026)020

[an] *Also at Millennium Institute for Subatomic physics at high energy frontier (SAPHIR), Santiago, Chile*
[ao] *Also at University of Chinese Academy of Sciences (UCAS), Beijing, China*
[†] *Deceased*

JHEP04(2026)020